



Integrated parametric design of adaptive facades for user's visual comfort

Amir Tabadkani^{a,*}, Masoud Valinejad Shoubi^b, Farzaneh Soflaei^c, Saeed Banihashemi^d

^a School of Architecture and Built Environment, Deakin University, Geelong Waterfront Campus, Australia

^b Department of building, civil and environmental engineering, Concordia University, Montreal, Canada

^c School of Architecture and Planning, Morgan State University, Baltimore, United States

^d Design & Built Environment school, University of Canberra, Australia

ARTICLE INFO

Keywords:

Hexagonal adaptive solar façade
Daylight performance
Discomfort glare
Visual comfort
Algorithmic simulation
Parametric design

ABSTRACT

The idea of Adaptive Solar Façade (ASF), as a modular, dynamic, and flexible types of smart façades could be a promising approach in a comfort-centric design through the proper integration with the parametric design. Therefore, this paper is to investigate the development process of ASF grounded on parametric design tools with a focus towards its visual comfort indices through a controllable shading system. To that end, first, a comprehensive literature review was carried out to develop an origami-based dynamic system, and three numerical timing patterns were then applied using Grasshopper plug-in for Rhino. In addition, the environmental plug-ins of Honeybee and Ladybug were employed to determine indoor daylight quality via different geometrical and physical properties. Thus, 1800 design models were prepared, based on several variables including rotation motions, indoor view angles, time hours and transmittance properties in order to investigate the daylighting performance and glare probability in a single office space located in the hot-arid climate representative; Tehran, Iran. Furthermore, interactive correlations between the geometrical pattern and visual performance were investigated, leading to this fact that the proposed prototype can significantly improve the flexibility of the shading system to control visual comfort. As the conclusion, all datasets were integrated into an algorithmic workflow while converting its advantages and limitations into an optimization process. Finally, a full potential hexagonal adaptive system was presented to achieve the maximum visual comfort level based on the users' preferences that can be the basis for future investment on smart building envelopes.

1. Introduction

This paper concentrates on the smart façade as an adaptive design technique in buildings, which is responsive to both direct environmental and human inputs; a concept that can be considered for the sustainable future. Studies have shown that buildings demand 34% of the world energy, which is even more than industry and transportation energy demands [50,51]. On the other hand, based on the Physical Institute in Maldegem, building façades are responsible for > 40% of heat loss in winter and for over-heating in summer that is making the employment of air conditioning systems necessary to guarantee an appropriate internal comfort [9].

It appears clear that the choice of the shading system typology is influenced by different factors: the geometry of the façade (planar or free-form façade), the design conception, the environmental efficiency, occupants, the technological performances and so forth. In addition to the architectural ambitions, several studies prove that some solutions are more efficient than others [9]. Nowadays, the idea of Adaptive Solar

Façade (ASF), as a modular, dynamic, and flexible façade, has been put forward by many scholars and designers around the world [3,12,30,35,56]. It has been defined as one of the most effective strategies to efficiently manage interactions between outdoor and indoor environments to maximize winter heating, summer shading and natural ventilation, acoustic insulation, transferring glare-free daylight and indoor comfort for occupants [5,52]. According to Hasselaar [25], climate adaptive skins should differ from conventional façades in a way that they are able to adjust their characteristics and mediate between the changing environments. By doing so, ASFs are capable of providing a comfortable indoor temperature, lighting level and air quality (parameters influencing energy consumption) without excessive usage of energy.

The transformable shading systems are aesthetically attractive while providing improved insulation across a window or other types of openings due to their modular construction. The design emphasis on various building structures has maintained pressure on the industry to continue creating unique aesthetically attractive coverings for

* Corresponding author.

E-mail address: stabadkani@deakin.edu.au (A. Tabadkani).

Acronyms

ASF	Adaptive Solar Façade
BBRI	The Belgian Building Research Institute
DA	Daylight Autonomy
DGI	Daylight Glare Index
DGP	Daylight Glare Probability
HOY	Hour Of the Year
hUDI	hourly Useful Daylight Illuminance
IES	Illuminating Engineering Society
SAD	Seasonal Affective Disorder
UDI	Useful Daylight Illuminance
UGR	Unified Glare Rating
VCP	Visual Comfort Probability
VLT	Visible Light Transmission

Nomenclature

A	Area, m^2
Td	Diffuse Transmission fraction, –
hUDI	Fraction of the task area within acceptable UDI thresholds, %
G	Glare, –

P	Guth position index, –
E	Illuminance, lux
L	Luminance, nit (or cd/m^2)
L_b	Luminance of the background, cd/m^2
$L_{s, i}$	Luminance of the i-th glare source, cd/m^2
L_s	Luminance of the source, cd/m^2
P_i	position index of the i-th glare source, –
$\omega_{s, i}$	Solid angle of the i-th glare source based on the viewing position of the observer, sr
ω	Solid angle of the source, sr
R_s	Specular Reflectance fraction, –
T_s	Specular Transmission fraction, –
S_r	Surface Roughness fraction, –
t	Time, hour
E_v	Vertical illuminance at eye level, Lux
wf	Weighting factor, –

Main subscripts

f	Floor
f, g, h	Empirical exponential coefficients
i	i-th

architectural openings. As some successful examples, Fig. 1 illustrates two different concepts of ASF where the energetic behaviour of the façade can be managed with high spatiotemporal resolution by separately addressable modules.

Previous studies revealed that different design methods towards efficient daylighting are one of the most important approaches employed in high performance contemporary buildings [36,58]. To maximize the benefit of daylight for individuals, it is necessary that indoor

design for daylight harvesting ensures occupants' visual comfort [22]. The natural light reduces the use of energy for artificial lighting, and that visual comfort is typically prioritized by users over concerns about energy efficiency for heating and cooling. Therefore, they will adjust shading devices based on their visual comfort sensation. In this regard, building fenestrations are responsible for daylight availability of indoor spaces, where designing a proper façade can enhance physiological and psychological needs [4,6,24].



Fig. 1. Examples of Adaptive Solar Façade (ASF) as an energy-saving design concept for a sustainable future (a, b) SDU University of Southern Denmark Campus Kolding, Denmark, by Henning Larsen Architects, 2014 (c, d) Al Bahr Towers complex in Abu Dhabi, United Arab Emirates, by: Aedas Architects, 2012 [16].

It has been also highlighted that exposure to the sunlight has a positive effect on the well-being and health of occupants by reducing some symptoms like headaches, depression, stress, eye strain and seasonal affective disorder (SAD) [1,49]. However, daylighting from openings can also bring unwanted reflections generated from a glare source that is a subjective sensation of visual discomfort, and has not been yet fully understood [53]. Although the introduction of transformable shading systems has greatly benefited the industry in this regard [2], there remains a need to create smart transformable shading systems having adaptability to climate change, and capability to be optimized based on visual comfort. While these parameters can directly impact illuminating or lighting effects perceived by occupants inside a subject unit, the shading system optimization can ultimately improve the annual energy consumption of the subject unit. Accordingly, there is a need for providing a responsive system for transformable shading system with motion flexibility to different timings and geometric adaptability. One of the most ambitious challenges for designers is to keep the balance between the daylight harvesting maximization on one hand, and magnitude of discomfort glare on the other hand [10]. Movable shading devices offer numerous benefits as these can be applied to allow for winter sun or to block direct summer sun. However, due to structural and budget reasons for the facades, high-rise buildings are generally constructed with glass curtain wall systems which could permit sheer volume of direct sunlight and solar radiation. Therefore, it is of value to utilize movable shading devices both to prevent and control undesirable daylight and solar radiation [28].

There are some studies carried out on the visual discomfort (glare) considering psychophysical factors [10,15,43,54,60], but the challenges to providing visual comfort as well as enhancing the energy efficiency in the glass-fronted (office) buildings still persist [19,23]. In this regard, the present paper specifically concentrates on the origami-based hexagonal facade as an adaptive shading system to user wishes in a single office unit in hot-arid climate representative; Tehran, Iran.

2. Research background

Having stated that adaptive façade is not a new concept for sustainable building skins; it has actually passed through different stages from the beginning of the 20th century [15,26]. In recent decades, there is a soaring trend in having glazed exterior façades for modern buildings, either entirely or predominantly glass. As a consequence, such transparency provides the undeniable physical and psychological health benefits like exposure to the sunlight and remarkable views. Albeit, the low thermal resistance of such facades means they are a step backward when it comes to the energy performance of building envelope [56]. Therefore, there have been considerable efforts towards the development of energy-conscious buildings by focusing on advanced adaptive systems [2,37,48]. The energy saving potential of these systems such as Electrochromic window has resulted in many applications [3], which can be adapted to changing climatic variability (daily, seasonally, or yearly).

The term of adaptive, here, signifies the potential to react or benefit from external climatic conditions in order to meet occupant comfort and well-being requirements [30]. As mentioned, this research focuses on daylight and discomfort glare based on a hexagonal ASF for the sustainable building design. In this context, daylighting is regarded as one of the main elements of space identification and quality which can play an important role in resource conservation, occupants' level of productivity, health and comfort [11,23]. As a further solution, daylighting systems may be integrated in the sustainable building facades that can be considered as a significant contributor to minimizing the need for artificial indoor lighting [45] and ensure visual comfort by controlling glare and patterns of contrast [42]. Visual comfort is explained as the state of mind that represents users' needs, preference and satisfaction with the visual indoor environment, impacting on mental and physical health [10]. It has been generally studied by the

evaluation of some factors affecting the correlation between the human needs and the indoor light environment including the amount, uniformity and quality of light in rendering colours, and the prediction of the risk of glare for users [29]. However, the mentioned parameters are possibly related with each other and an index-based study usually concentrates on only one of them [38].

As one of the comprehensive example, a study was carried out by Carlucci et al. [13] on the visual comfort and daylight integration, according to a list of 34 indices to assess the visual comfort. It was indicated that most of the collected indices are assigned to evaluation or prediction of 1) glare (17/34; 50%), 2) the amount of light (9/34; 26%), 3) the light quality (7/34; 21%), and 4) the light uniformity (1/34; 3%). Hafiz [23], also mentioned that there are key factors such as orientation, sky condition, and climate characteristics, which need to be considered when applying a daylighting and visual comfort study.

Another study on present indices affirmed that UDI is one of the most appropriate factors for evaluating the effects of daylighting on visual discomfort [21]. Furthermore, "DGP is the only index based on vertical eye illuminance and hence it is strongly linked to the occupant's lighting perception during that time" [21], to make comparison of various design scenarios and control solutions. In detail, DGI is another index in the building simulation and solar radiation control, and it can be adopted in case of evaluating the effect of glare under uniform large sources. Collectively, Mardaljevic et al. analyzed different indicators and recommended analyzing three factors of UDI, DGP and DGI. However, the correlation among these indicators and the reliability of the associated assessments are in question [32]. It was also suggested that employing these indicators via a collective analysis could provide more comprehensive results [31].

Henceforth, in the present study, the UDI, DGP, and DGI are considered as the main indices to assess the visual comfort in a south-faced office unit, as follow:

- i. UDI: This indicator is used for evaluation of the light amount that is available in a specific space; an attempt to integrate the evaluation of daylight level and glare in one scheme. It is explained as the annual time fraction that indoor horizontal daylight illuminance at a given test point reaches in a given domain. UDI is a two-tailed metric that contains lower and upper thresholds and an acceptable range as $UDI_{underlit}$, $UDI_{overlit}$ and UDI_{useful} respectively [15] (Eq. (1)). However, according to the literature, different limit values have been proposed based on the researchers' priority [53].

$$UDI = \frac{\sum_i (w_{f_i} \cdot t_i)}{\sum_i t_i} \in [0.1]$$

$$\left\{ \begin{array}{l} UDI_{Overall} \quad \text{with} \quad w_{f_i} = \begin{cases} 1 & \text{if } E_{Daylight} > E_{Upper\ limit} \\ 0 & \text{if } E_{Daylight} \leq E_{Upper\ limit} \end{cases} \\ UDI_{Useful} \quad \text{with} \quad w_{f_i} = \begin{cases} 1 & \text{if } E_{Lower\ limit} \leq E_{Daylight} \leq E_{Upper\ limit} \\ 0 & \text{if } E_{Daylight} < E_{Lower\ limit} \vee E_{Daylight} > E_{Upper\ limit} \end{cases} \\ UDI_{Underlit} \quad \text{with} \quad w_{f_i} = \begin{cases} 1 & \text{if } E_{Daylight} < E_{Lower\ limit} \\ 0 & \text{if } E_{Daylight} \geq E_{Lower\ limit} \end{cases} \end{array} \right. \quad [15] \quad (1)$$

The range considered "useful" is based on a survey of reports of occupant preferences and behaviour in daylight offices with user operated shading devices. Daylight illuminance from 300 to 3000 lx is often perceived either as desirable or at least tolerable. Carlucci et al. [13] and Hafiz [23], also defined UDI as the illuminances that fall within the range 100–2000 lx based on data from comprehensive field studies of occupant behaviour.

- ii. DGI: According to Hafiz [23], glare is the difficulty in the sight

subject to the presence of bright light resulting from a direct or reflected light source in the visual field. It is typically represented as the ratio of the size, position, and luminance of glare sources in view field, when compared to the average luminance regardless of the glare source. Kurnia et al. [29] mentioned that indoor glare is quantified in a single space by using the concept of glare index, which is a quantitative measure to evaluate the amount of glare perceived by the observer in different view angles. Generally, it can be formulated by the following equation:

$$G = \left(\frac{L_s^e \cdot \omega_s^f}{L_b^g \cdot f(P)} \right) [29] \quad (2)$$

Since this equation is generic; thus, further studies are required to determine the appropriate glare index formula according to empirical data. As the seminal study, Hopkinson [26] defined DGI as the possibility of a large amount of glare source, particularly from the diffuse sky visible across a window. However, it presents some noticeable limitations and difficulties [10]: (i) it excludes the direct sunlight and only refers to uniform sources while non-uniform sources can result in higher discomfort glare when they are positioned perpendicularly to the user's view field [54]; (ii) DGI is not reliable when the source covers the whole view field and if the background luminance is equal to source illuminance; (iii) as stated in literature [55], there are differences between DGI value and real sky conditions. Hopkinson [26], derived DGI formula from subjective perceptions, and according to the research results, $DGI > 31$ indicates intolerable glare, and $DGI < 18$ shows that the glare is barely perceptible. While values higher than 24 put user's visual field in the uncomfortable range. The DGI equation is as follows:

$$DGI = 10 \log_{10} \left[0.478 \sum_{i=1}^n \left(\frac{L_{s-i}^{1.6} \cdot \omega_{s-i}^{0.8}}{L_b + 0.07 \omega_{s-i}^{0.5} \cdot L_{win} \cdot P_i^{1.6}} \right) \right] [26] \quad (3)$$

iii. DGP: It is defined as the percentage of people bothered by the level of discomfort glare. This method is a relatively new approach for glare prediction, an empirical approach based on the vertical eye illuminance (E_v) rather than background luminance (L_b). It considers the overall brightness of the view, position of glare sources as well as visual contrast, in order to provide a powerful connection to the user response concerning glare sensitivity when compared to other existing glare studies [23]. This method was proposed by Wienold and Christoffersen in 2006 in which, it includes vertical illuminance on the observer's eye in addition to the luminance contrast component [60]. In comparison with the other glare indices, this method has a higher correlation with the subjective perception of discomfort glare, because of the inclusion of the vertical illuminance component [29]. Wienold and Christoffersen [60] suggested the following glare comfort criteria for DGP in which $DGP < 0.35$ is meant to represent 'imperceptible' glare, $0.35 < DGP < 0.40$ is perceived as 'perceptible', $0.40 < DGP < 0.45$ is meant to represent 'disturbing' and lastly, $DGP > 0.45$ is considered as 'intolerable'.

$$DGP = 5.87 \cdot 10^{-5} E_v + 0.0918 \cdot \log_{10} \left[1 + \sum_{i=1}^n \left(\frac{L_{s-i}^2 \cdot \omega_{s-i}}{E_v^{1.87} \cdot P_i^2} \right) \right] + 0.16 [29] \quad (4)$$

In a nutshell, the comprehensive literature review on three key ideas of adaptive façade, daylight performance, and visual comfort illustrates that although the literature is replete with the studies on the daylighting in different building types, the concept of sustainable façade as an adaptive building system is undermined [35]. With this respect, ASF exploration could be developed via folding the surface, exploring crease patterns and applying active materials as actuators. Therefore, the hypothesis of this research lies in their combination with the origami technique to create a system whose displacements are compatible with façade applications. Such an application of the origami fits the patterns into different reconfiguration structures. However, applying self-folding ASF in architecture falls to the generally experimental approaches in shading devices and façade applications. This trend in shading device studies is to shift from traditional mechanical systems with multi-functional and smart actuators [33].

In fact, developing kinematic and hexagonal ASF is employed to rectify the errors of traditional louvers thanks to the dynamic nature of these patterns. Passing different angles through folding/unfolding presents a louver-like behaviour capable of managing incoming radiations during a year [40]. Furthermore, the spontaneous self-organization of hexagonal geometries is the intuitive way to deliver adaptation. By virtue of tessellation's creases, these shapes make the ASF to deform by pre-fixed deformation directions in the meanwhile of being fixed in the other directions. Hence, these systems benefit from altering their shapes to conform with new situations while maintaining a continuous external surface [39].

Such a system is able to transfer glare-free daylight into the interiors in order to provide visual comfort for occupants. This is particularly applicable to the glazed office buildings where the daylight presence for indoor illumination impacts on the satisfaction, health and well-being of employees has only received limited appraisal in architectural scholarship [36]. Analysis of the hexagonal geometrise in ASF can be done by applying generative processes in understanding the kinematics behind this type of movements. Tessellations and geometric patterns can be created by arranging hexagons regularly arranged into a matrix. That is why generative algorithms of parametric design are necessary in setting up rules to generate the modules and then apply these rules to the object. Furthermore, digital software is required to control variables through a parametric design that can be updated step-by-step development of dimensions, deformation strength and degrees of control [20].

Thus, this research goes further to fulfil this gap by developing a computerised model based on evaluating glare comfort in different visual fields. It is also designed to maximize UDI via a hexagonal responsive skin as a dynamic shading system through DGP and DGI metrics, in three different occupants' view angles.

3. Research methodology

The ultimate goal of this research is to present a hexagonal ASF as an innovative modular and highly integrated with the dynamic building system which considers user demand. To that end, the main

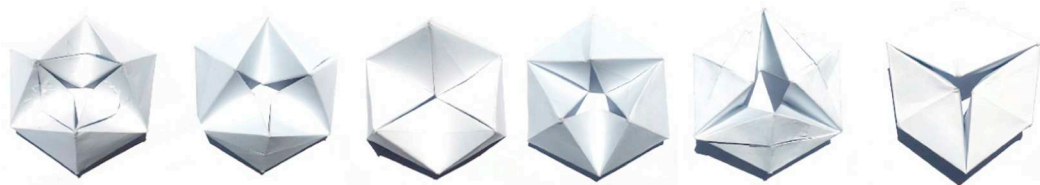


Fig. 2. Origami-inspired concept to design of hexagonal ASF.

architectural idea for designing the prototype, was inspired by Origami and paper pleating techniques. Applications of kinetic origami and folding concepts were used repetitively in modular large-scale facades [17] which illustrate the ability of controlling the structure through moving parts. In addition, some origami and paper pleating techniques were also designed into the kinetic solar screens that present an efficient solution to reduction of heat load, while providing appropriate daylighting for interior spaces [34] (Fig. 2).

Origami evolution was studied regarding different skin components, and defined as the transformation of arrangement and geometry of individual kinetic parts as well as the motion of control means between them [55]. Origami offers a finite set of paper-folding techniques that can be catalogued and tested with parametric modelling software [40]. This research focuses on optimizing the divisions and number of folds and its movements; a way to achieve various deployable façade shading devices classified by different factors, which define the strengths and weaknesses of each tessellation. It examines the possibilities of different arrangements of folded modules to create environmentally efficient kinetic morphed skins, and aims to achieve different kinetic origami-based shading screens categorized by series of parameters to provide the appropriate visual comfort. To link the parametric design approach to indoor visual environment, computational tools can be applied effectively to assess qualitative and quantitative aspects of optimizing a prototype once it is formed [35]. Therefore, this research presents an algorithmic and parametric-based design approach developed in

Rhino/Grasshopper as a parametric modelling tool. Grasshopper is a plug-in for Rhinoceros 3D modelling software and is a graphical algorithm editor that allows designers to generate parametric forms, ranging from the simple to the complex modules without scripting experiences [7]. Meanwhile, parametric software was used to combine different dimensions and proportions to simulate shape kinetics, daylight and glare analyses considering the pattern variations during the year. To that end, the weather file has been imported via Ladybug plug-in and Honeybee [44] has been employed to run the environmental simulations by allowing the user to connect Daysim® and Radiance® for visual comfort analysis.

Fig. 3 illustrates the organization of the research flow and methodology of this study. As discussed, the study begins with a folding technique inspiration which leads to a kinetic structure and a hypothesis based on available studies in this field. The hypothesis conducted through quantitative method via integrating algorithmic approach towards simulation stage in a back and forth loop. The possibilities and limitations of creating the ASF within algorithms are explored in a practical case study via a side-lit south-facing single office space, located in Tehran; Iran as a case study, in three consecutive phases as follow:

- i. The first phase investigates the kinetic behaviour of a Timing-based hexagonal Kaleidocycle pattern, which is an acclimated shading device to control daylight uniformity via computational design tools

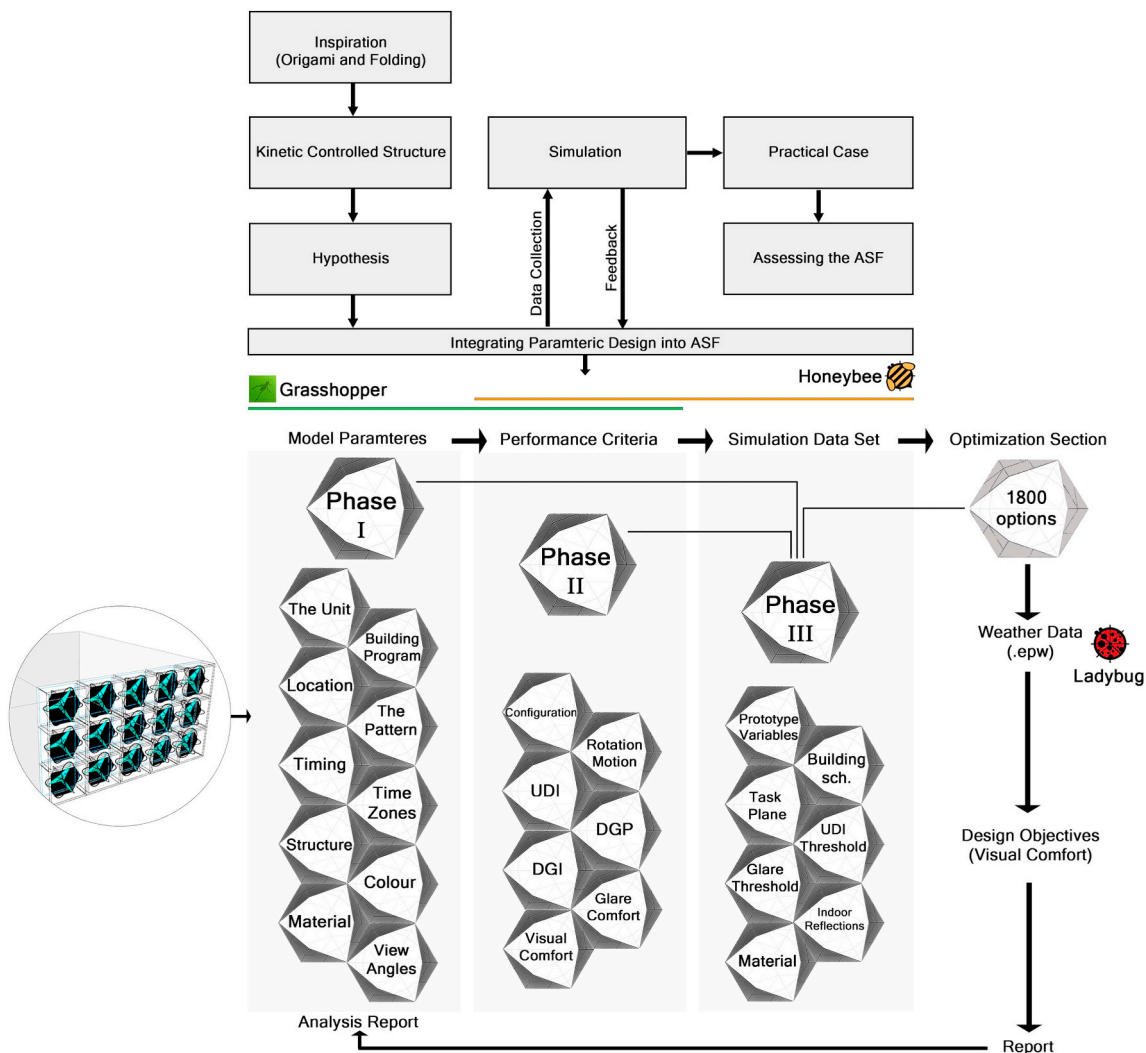


Fig. 3. Research design.

of Grasshopper/Rhino.

- ii. In the second phase and in parallel with parameterized prototype, a list of critical daylight and glare indices that leads to indoor visual comfort performance of the case study is developed through optimization capabilities of Grasshopper. This phase is progressed by Honeybee plug-in and dedicated to daylight performance and glare probability via its integration with Radiance and Daysim.
- iii. In the third phase, based on the input variables, the algorithm generates all the possible simulation datasets via an evolutionary solver function called Galapagos which is a genetic algorithm framework embedded within Grasshopper to find optimum solutions of the generations [46]. It associates with a feedback loop to the initial phase to reconsider the design variables if necessary, to meet the final fitness.

3.1. The first phase: model parameters

In the office-type environments, where occupants typically cannot freely adjust their position and have restricted visual comfort alternatives, the building skin plays a significant role to provide sufficient indoor daylight using either smart façade orientations or automated shades. In this regard, the process starts considering configurations of a hexagonal Kaleidocycle module that was applied to a completely glazed south face of an office space having Window to Wall Ratio (WWR) of 81% with spatial dimensions of 5.5 m (width), 7 m (depth) and 3 m (clear height) as illustrated in Fig. 4. The measured space is 7 m deep to give the opportunity to clearly test the oriental skin efficiency.

The proposed hexagonal Kaleidocycle skin is formed from six repetitive arrays of Kaleidocycle ring, which is a mix of triangular and hexagon patterns. Each module has shown the potential to deliver an interesting rate of the rotation motion and geometrical proportions that are fitted in a regular set of frames to cover the whole glazed façade and ensure hexagonal structural performance. This system is configured to automatically transform into different geometries in response to user preferences. In the Fig. 5, the modular unit can include a plurality of structural rings (NO.12), a plurality of deployable shell panels (NO.16 and 22), a plurality of structural pipes (NO.18), and a plurality of gear boxes (NO.24 and 14). In one implementation, the plurality of the structural rings can include, for example, six structural rings, and a surrounding rail. The plurality of deployable shell panels may have a first group (NO.16) including six deployable shell panels, and a second group (NO.22) of six deployable shell panels. Two deployable shell panels forming the first and second groups can be positioned within each of the six structural rings of the modular unit. The plurality of structural pipes may be configured to define a margin of each of the deployable shell panels. In an aspect, the plurality of structural pipes of each of the deployable shell panels can be formed of flexible materials including plastics or cloth textures. The area of deployable shell panels (NO.16 and 22) are variable in different positions that the system can support based on a non-linear behaviour. Therefore, an especially designated algorithm was written to provide a wide range of orientations via a Timing Position Pattern that enables hundreds of motions to control the daylight and glare, simultaneously.

The plurality of the deployable shell panels (NO.16 and NO.22) may expand in the two-dimensional representation in which each of the plurality of the deployable shell panels in the first group (NO.16) is

associated with each of the plurality of the gear boxes in the first group (NO.24). Likewise, each of the plurality of the deployable shell panels in the second group (NO.22) is associated with each of the plurality of the gear boxes in the second group (NO.14). In an aspect, a structural connection between each of the plurality of gear boxes (NO.24 and NO.14), and the plurality of deployable shell panels (NO.16 and NO.22) are described in more details in Fig. 6. It illustrates an exemplary structural connection that can be configured to connect each of the plurality of the gear boxes to the plurality of the structural pipes of the deployable shell panels (NO.16 and NO.22). The connection (NO.50) may be configured to function as a hinge, and to allow the gear boxes freely adjust an angle between the gear boxes and the plurality of the structural pipes in response to different geometric transformations. This is the position where the first group (NO.16) and the second group (NO.22) of the deployable shell panels can be formed of flexible materials such as natural rubber or highly flexible polyurethane, which can support all positions and geometries.

Accordingly, three patterns are proposed to apply on kinetic Kaleidocycle modules. Each circular ring also contains of two gear boxes as joints that can move along its path based on the selected Timing curve to shape a three-dimensional hexagonal geometry. In an aspect, a structural positioning of the gear boxes within the surrounding rail of each of the structural rings, and a timing motion of such gear boxes in respect to one another can selectively change based on a user's need. Progressively, the structural positioning and the timing motion of the gear boxes in turn may command each of the deployable shell panels within each of the structural rings to transform into a separate geometry, in which each geometry can be applied to one specific geographical positioning and system functioning. In a related aspect, the gear boxes may be configured to work with dc power supply of 12 v and the rotational frequency of 50 rpm. The timing pattern allows the user to find indoor visual environment in an acceptable range for the office space and providing the daylight and glare control manageable. Thus, during the preliminary simulations, the combination of three-dimensional nature of the hexagonal system and timing curves were proved difficult to compute properly. In order to avoid geometric issues with the ray-tracing algorithm and obtain reliable data within wide range of possible pattern configurations, the timing pattern positions have been simplified into 6 individual positions for each case that are shown on the timing curve graph in Fig. 7. The gear boxes are shown by red dots and their positions are adjustable based on the applied timing behaviour in the system. Accordingly, by changing the speed and place of gear boxes with each other, daylight and glare can be controllable on the base of users' demands.

The primary concept of the developed parametric model is the joints displacements based on the timing curves, where the central hole periodically disappears or the triangular patterns can be centralized to control excessive unwanted daylight. This happens through adjusting the angular dimensions between joints (Fig. 8), which can be further optimized to enhance the indoor visual comfort. Since the individual module is defined by adjustable parameters, changing the numerical values associated with timing curve and joints placement can result in different Kaleidocycle rotations following the timing curve trends (Fig. 8).

As mentioned in the research background, the visual comfort has different dimensions to evaluate. In addition to the kinetic reaction of

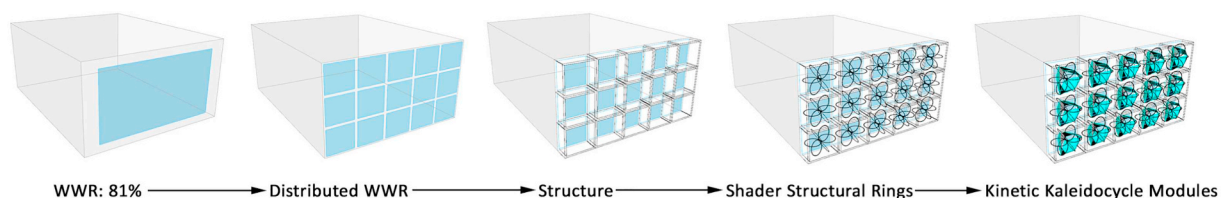


Fig. 4. Modelling process.

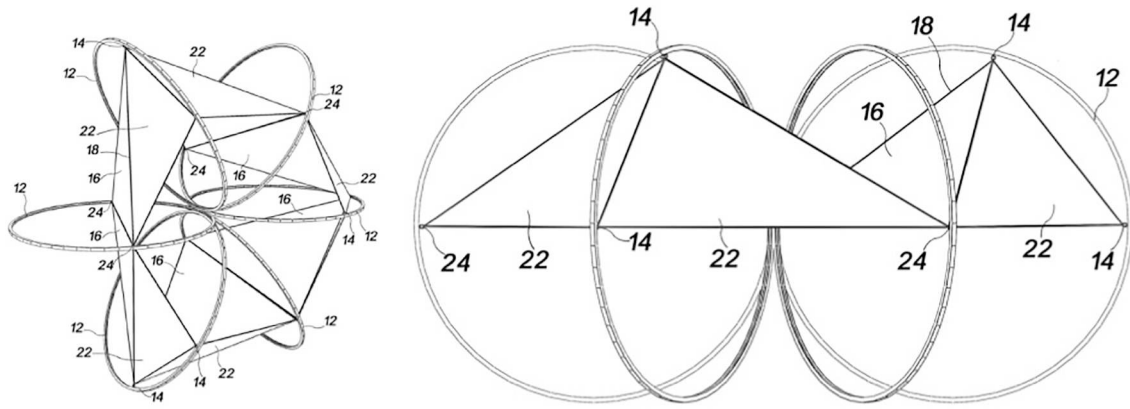


Fig. 5. Modular unit (adapted from [57]).

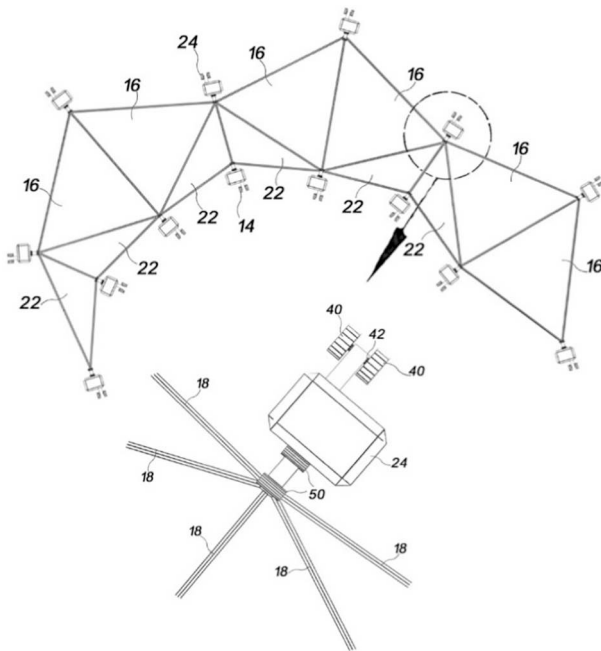


Fig. 6. Modular unit (adapted from [57]).

the system, material settings play a significant role in daylighting and glare control that could result in visual comfort or discomfort. There are two types of physical properties options that are assigned in this research flow. The first group includes the generic materials having outside ground, window and its frame, interior ceiling, walls and floor that corresponds to office room besides structural rings related to the Kaleidocycle modules. The second group consists of the customized translucent materials to permit daylight penetration applied to south-faced hexagonal Kaleidocycle patterns as a variable. In order to create a realistic scene, all the interior main surfaces have been assigned based on the European Standard [14] as indicated in Table 1.

Considering hexagonal modules and their oriental motions, the suggested materials should have a flexible and transmittance characteristic as to stretch and fold easily while allowing the daylight enters the indoor space. Thus, in this research, there are two textures as the 1st and 2nd modules which are shown by bright blue and grey colours in Fig. 8, respectively. These modules have been individually associated with five different sun shade fabrics [27] to test their features in enhancing daylight performance and minimizing discomfort glare. Consequently, selected customized materials for hexagonal Kaleidocycle patterns are presented in Table 2.

After setting sun shade properties, the algorithm was synchronized to be imported into a grid-based daylight simulation component in Honeybee Plug-in for Grasshopper. This is to compute the fraction of the task area within acceptable UDI thresholds as hourly Useful Daylight Illuminance (hUDI) and glare comfort range in the second

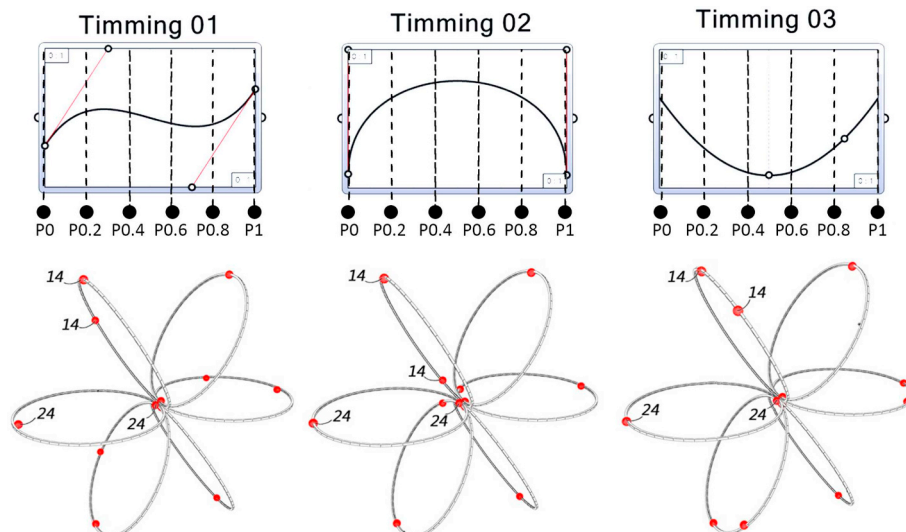


Fig. 7. Timing patterns.

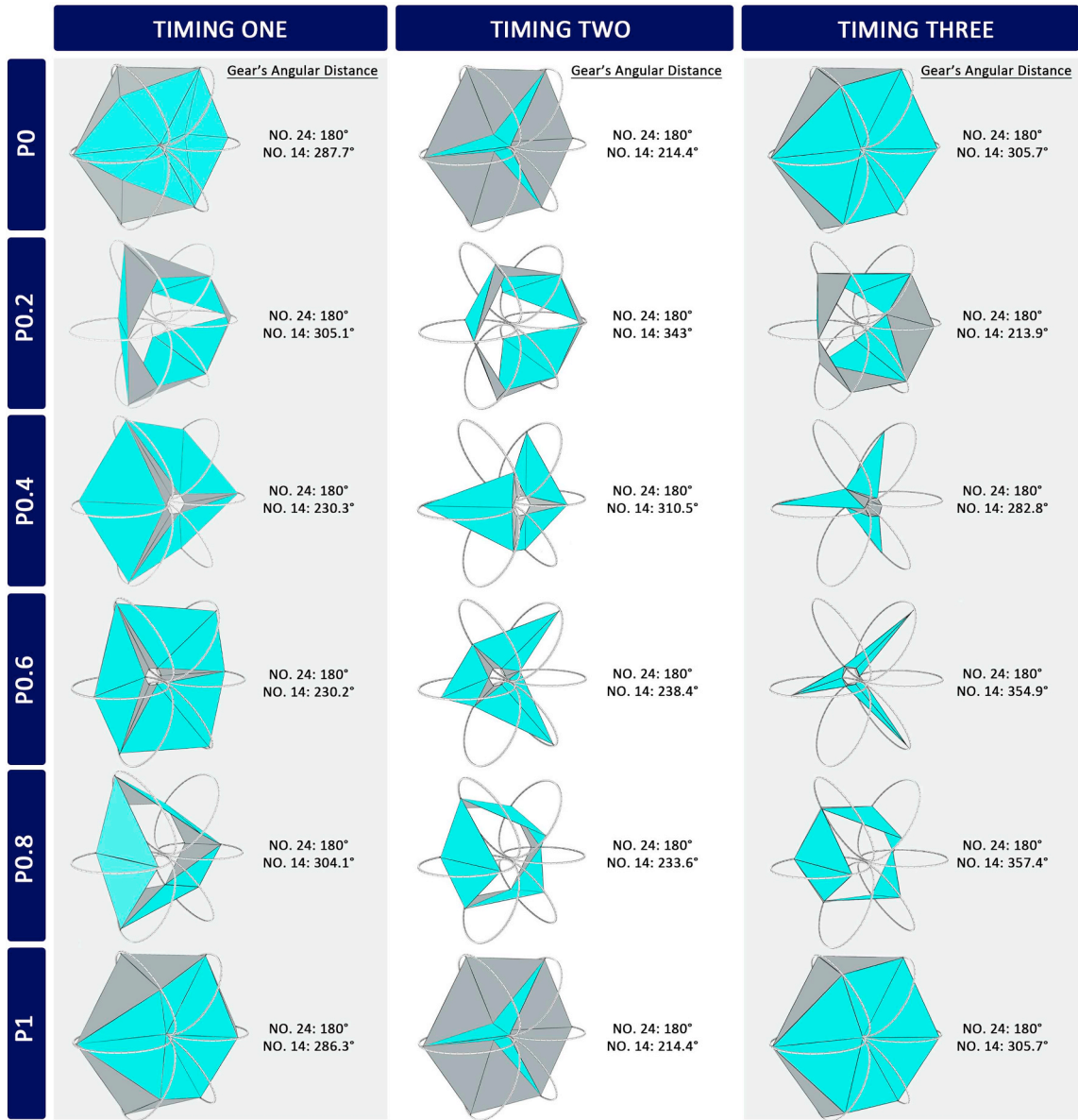


Fig. 8. Hexagonal Kaleidocycle patterns vs. timing positions.

Table 1
Generic materials.

Outdoor surface	
Outside ground	20% reflectance
Indoor surfaces [14]	
Interior walls	50% reflectance
Interior ceiling	80% reflectance
Interior floor	20% reflectance
Glazing surface and the Kaleidocycle modules	
Window	70% transmission (double pane window)
Frame	10% reflectance
Rings	10% reflectance

phase.




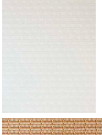

3.2. The second phase: performance criteria

The essential aim of this phase is to analyse the influence of the adaptive system in terms of its three-dimensional motions and material

properties to control the indoor illuminance and glare possibility. To this purpose, Honeybee environmental plug-in for Grasshopper was used to investigate the daylight performance of each hexagonal Kaleidocycle configuration, and its physical features to meet visual performance. Honeybee provides the advanced grid-based daylighting mode grounded on the UDI threshold in which it allows the designer to control skin layers according to the amount of light on the elevated task area with 85 cm height in this research [56]. Additionally, the algorithm also enables the user to calculate glare indices as the main performance criteria via considering background luminance, view to exterior, contrast to the field of views regarding materials reflectance and colour (Fig. 9). This figure clearly distinguishes the daylight vis-à-vis glare analysis grounded on different performance criteria they have, as mentioned.

As Fig. 10 illustrates, the parametric model provides a constant feedback on the explorations of the proposed scenarios of Kaleidocycle system by setting thresholds for illuminance and glare indices. In the meanwhile, hourly daylight and glare simulations convert possible configurations into numerical values to measure visual comfort performance. Furthermore, the main driving parameters are kinetic

Table 2
Assigned material definitions for Kaleidocycle modules (adapted from [27]).

Code	Name	Image	Type	Openness factor/VLT	Material description	Measures
0	Mesa-beige		Translucent	10%/16%	RGB reflectance (RGB): depends on colour	RGB: 0.32 - 0.67 - 0.04/ Rs: 0/ Sr: 0.02/ Td: 0.295/ Ts: 0.625
1	Mesa-oyster		Translucent	1%/13%	Specular reflectance (Rs): surface specularity has been considered equal to zero	RGB: 0.31 - 0.78 - 0.07/ Rs: 0/ Sr: 0.02/ Td: 0.212/ Ts: 0.077
2	Palmetto-black		Translucent	8%/8%	Surface roughness (Sr): almost zero	RGB: 0.08 - 0.18 - 0.18/ Rs: 0/ Sr: 0.02/ Td: 0.537/ Ts: 1
3	Season-white		Translucent	0%/17%	Diffuse transmission (Td): fraction transmitted diffusely in a scattering fashion	RGB: 0.35 - 0.88 - 0.08/ Rs: 0/ Sr: 0.02/ Td: 0.245/ Ts: 0
4	Natural-rattan		Translucent	7%/12%	Specular transmission (Ts): fraction transmitted as a beam	RGB: 0.33 - 0.75 - 0.04/ Rs: 0/ Sr: 0.02/ Td: 0.2/ Ts: 0.583

Kaleidocycle patterns based on the timing position, material specifications, and motion scenarios as applied in Honeybee/Grasshopper algorithmic process, three different view angles, and assuming seasonal time hours during a year. As a result, the optimization includes 1800 generations as decision-making strategies based on the given visual comfort dataset in the third phase.

3.3. The third phase: simulation data set

In order to evaluate the trend of the selected daylight and glare parameters obtained from the performance criteria, simulations for each skin configuration have been performed in four extreme and mediate time hours. This is to cover all possible time intervals [18]: 21st of March, June, September and December at 12 P.M., which are represented respectively as Hour Of the Year (HOY): 1908, 4116, 6324

and 8508 when the sun position reaches the most perpendicular angle to the facade. Analysis and simulation of adaptive skins and the dynamic test of their visual performance are a challenging issues in a parametric approach. The third phase covers the analysis of the developed Kaleidocycle kinetic skin in applying the angular transformations in response to the daylighting and glare measures. This happens in the meanwhile of searching for optimal solutions with required indoor illuminance and minimum glare risk among generations. Therefore, the aim of this phase is to propose a dynamic screen rotation angles that can be adjusted to improve occupant visual environment at the tested hours while printed in the Microsoft Excel spreadsheets.

This is performed by conducting a problem solving exhaustive method through Galapagos, an evolutionary solver in Grasshopper known as a genetic algorithm, which is the most common optimization tool used in the parametric design [8] (Fig. 11). Galapagos presents a

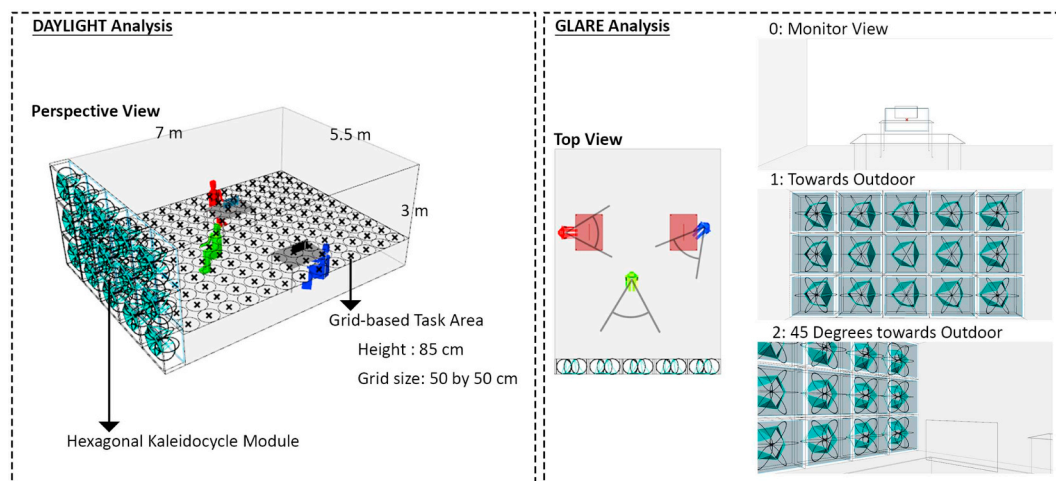


Fig. 9. Daylight vs. glare analysis.

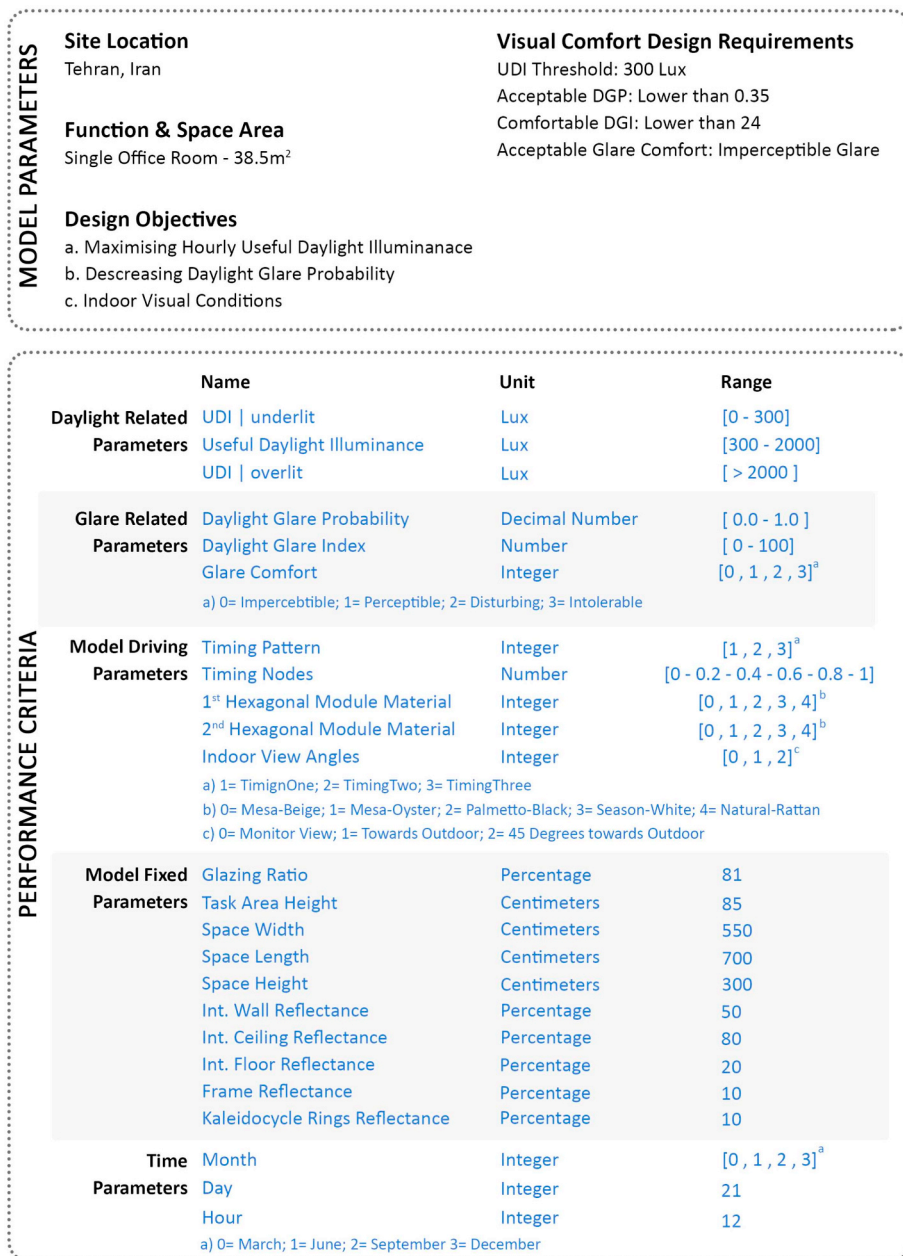


Fig. 10. Model parameters and performance criteria of the procedures towards simulation.

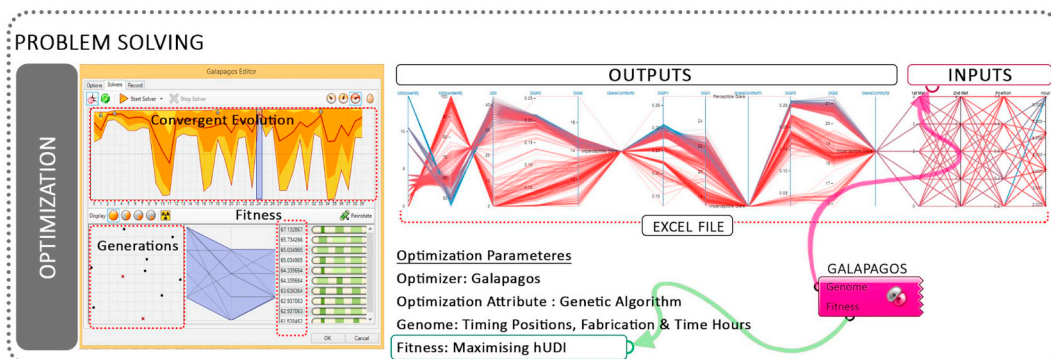


Fig. 11. Parametric optimization.

fitness landscape where the valleys represent low-quality states and peaks represent solutions. However, this landscape is abstract and not fully computable due to the time limitation. Hence, this should be constrained to sampling a minority of phase-space locations in the meantime of yielding an acceptable solution. This is what Galapagos generic solver is supposed to be good at. It finds high ground in uncharted fitness landscapes. Having stated that there is no guarantee to identify the best solution in a finite amount of time and resource [47]. In order to guide simulations towards optimal design solutions, the fitness function was set to maximize hUDI.

Max stagnant was empirically fixed on 100 iterations for the initial population of 35 generations of genomes. This rule means if the fitness of 100 consecutive iterations comprising 35 generations of 3 genomes is kept fixed, the evolutionary solver function is terminated [56]. To control the distance of genomes in each generation, the inbreeding rate was determined on 75% and the digital variant was maintained on 3%. This rule indicates how the relative offset of genomes (parameters) could be guided in distributing the mutation and crossing over of parameters for securing an appropriate functional handling in dataset generations [7]. The parametric problem solver contains an engine to find the optimum solutions of the Kaleidocycle variables, where the optimized samples were defined in two methods: obtaining the required daylight illuminance threshold by 300 lx and decreasing the glare risk in all view angles.

4. Results and discussion

A synthesis of the results that were obtained from the proposed integrated approach is presented in this section, with reference to the performance criteria and simulation data sets based on the medium rendering quality due to the time and hardware limitations (Table 3). The daylight simulations and glare risk in the field of views were employed by inputting hourly weather data of Tehran, Iran, where an

adaptive skin model was developed for a south-oriented workstation in the office unit, exposed to the direct sunlight with Standard CIE sky; intermediate with Sun (Table 3). The selected sky condition was initially analyzed through Ladybug tool to evaluate the amount of sky dome coverage by clouds or obscuring phenomena at the hour indicated over a year as a fraction of total sky coverage (minimum value:0; maximum value:10), where the average value is 4.47 out of 10 which shows that around half of the year is covered.

Moreover, the main model properties regarding the reflectance measurements for generic envelope, hexagonal Kaleidocycle prototype, and physical transformations based on the timing trends, are addressed in Figs. 9 and 11. In order to clarify the parametric analysis, all of the possible generations and related results were categorized into three main sections to discuss, as follow:

- Exporting design variations to the Microsoft Excel spreadsheets, to illustrate the filtered solutions via Design Explorer application, which is an open source tool for exploring multi-objective parametric studies [59].
- Verifying the timing-based model according to the maximum indoor illuminance for each tested hours, while considering the skin configuration and its fabric settings.
- Analyzing the glare discomfort outputs for individual view fields based on the obtained point-in-time UDI and Timing patterns.
- Comparing selected shading states with an unshaded condition and conventional system (venetian blinds) in order to evaluate their performance within a simulation-based process in a higher rendering settings.

4.1. Optimization dataset

As a part of results, an optimization algorithm was created according to medium simulation settings (Table 3) [41], reading the

Table 3
CIE sky condition.

Hourly sky condition of Tehran, Iran

Hourly sky condition of Tehran, Iran

12 AM

6 PM

12 PM

6 AM

12 AM

Jan

Feb

Mar

Apr

May

Jun

Jul

Aug

Sep

Oct

Nov

Dec

Total Cloud Cover (tenths) - Hourly
Tehran Mehrabad, IRN
1 JAN 1:00 - 31 DEC 24:00

Direct and diffuse radiation of the sky (based on weather file)

	Direct	Diffuse
21 st March 12 P.M.	485	422
21 st June 12 P.M.	666	417
21 st September 12 P.M.	761	305
21 st December 12 P.M.	437	255

Medium rendering settings (adapted from [41])

Ambient bounces: 3 – ambient division: 512 – ambient resolution: 32 – ambient accuracy: 0.25 – ambient super-samples: 128

Direct and Diffuse radiation of the sky (based on weather file)

	Direct	Diffuse
21 st March 12 P.M.	485	422
21 st June 12 P.M.	666	417
21 st September 12 P.M.	761	305
21 st December 12 P.M.	437	255

Medium Rendering Settings (adapted from [41])

Ambient Bounces: 3 – Ambient Division: 512 – Ambient Resolution: 32 – Ambient Accuracy: 0.25 – Ambient Super-samples: 128

detailed output of Honeybee, and applying the genetic algorithm approach. This is in light of an objective to maximize useful daylight of the task area fraction by obtaining the ordered daylight performance as well as the corresponding indices of discomfort. Moreover, a complementary online software 'Design Explorer' was applied to analyse multi-objective behaviour of the prototype and break down the results for better understanding. Therefore, with respect to the evaluation of the overall skin efficiency, several sub-objectives were extracted for each design solution as the below:

- UDI in three domains: UDI, UDI_{overlit} and UDI_{underlit}
- DGP, DGI and Comfort range for individual view angles (Glare Comfort)
- 1st and 2nd modules of material types based on Table 2
- Timing Positions (P0, P0.2, P0.4, P0.6, P0.8, P1)
- Time hours (HOY: 1908, 4116, 6324, 8508)

Following the above optimization dataset, one of the selected outputs with the modified input sliders is shown in Fig. 12 which applies to the conditions studied for Timing Two experiment. It shows the correlations between UDI domains and Glare indices (DGP and DGI) within three view fields depending on variable expressions via applying individual filters on total generations. As shown in Fig. 12, low illuminance known as UDI_{underlit} domain starts from 45% to a complete shaded area < 300 lx, where user can experience it in all selected hours in cases if the shading position remains constant at P1. Desired illuminance intensity between 300 and 2000 lx covers up to 40% of the

elevated task area in hours 1908, 6324 and 8508 since proposed timing positions and their openness factor is relatively high, although the users' view fields remained in comfortable range as discussed in Section 4.3. UDI_{overlit} ranges from 0 to 15% in all generations which in December (HOY: 8508), due to the lower sun altitude, the incoming daylight magnitude of 2000 lx reaches 14% of the task area, and sunlight penetrates deep in to the end of the room, as shown in Fig. 13. Moreover, except for June that tested configurations played a significant role in shading interior, there are few optimum solutions that could address the main visual comfort requirements. It is constrained to the minimum of 50% of the task, where Positions 0.2 and 0.4 of Timing Two can be selected as the most favourable configurations, however it depends on the user preference during working hours.

4.2. hUDI and timing patterns

The next contribution of parametric analysis lied in generating design models for the internal daylighting conditions, and consequently adjusting the hexagonal adaptive system for the visual comfort of occupants. Fig. 13 illustrates the results related to the selected and available maximum illuminance during selected time hours of the year regarding the individual timing patterns, as a part of research process.

Furthermore, the hUDI is also represented, as a fraction of the task area, which has achieved within the defined range (> 300 lx) in percentage. Therefore, in order to provide a precise decision-making process of this section, the results are separated based on the Timing Patterns and the selected Time Hours respectively, as follow:

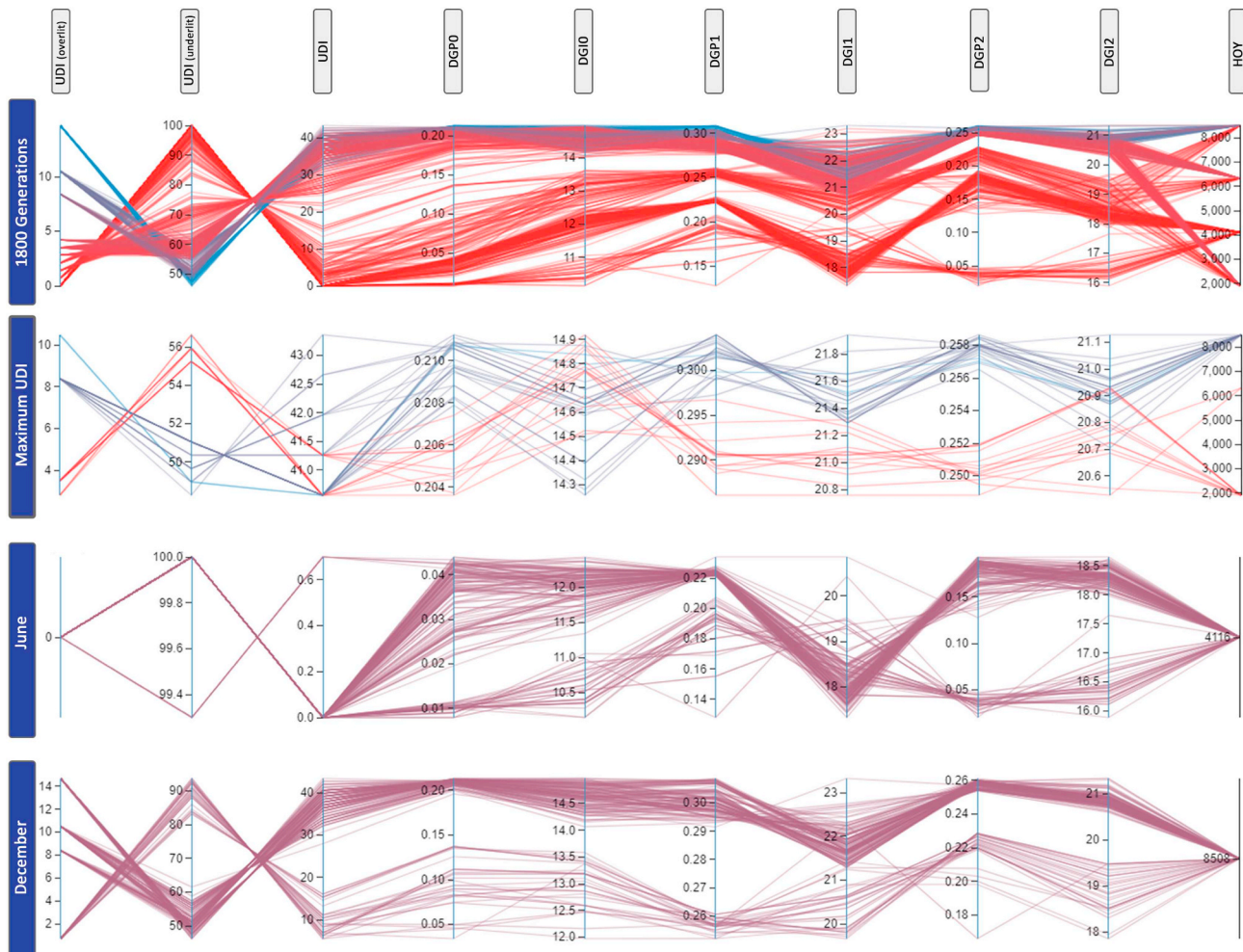


Fig. 12. Optimization outputs (Timing Two) (Timing One: <https://bit.ly/2V2YTAf>; Timing Two: <https://bit.ly/2PNBLEA>; Timing Three: <https://bit.ly/2DR3MGC>).

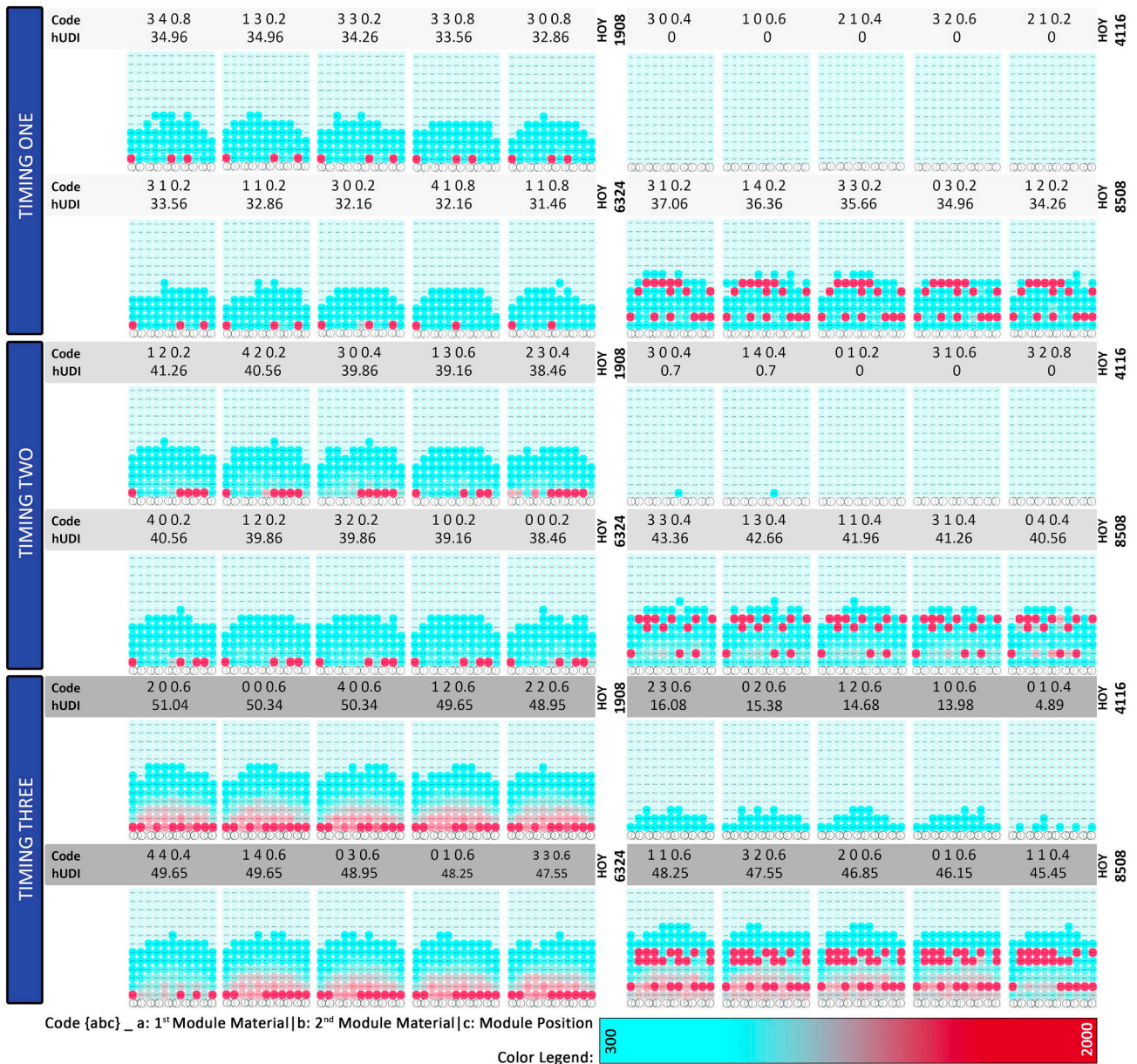


Fig. 13. Hourly daylight performance vs. timing modes.

- i. Timing One: The maximum fraction of indoor illuminance can be achieved by the task plane when the timing position maintained at P0.2 with numerical values of 37.06 in 21st of December at noon (HOY: 8508). Furthermore, in June, none of the design solutions is in the acceptable illuminance threshold, but the lower level of incoming sun rays can provide a shading opportunity in summer time.
- ii. Timing Two: The achieved hUDI presented higher performance in March, September and December regarding the patterns and positions of Kaleidocycle in which the opening fraction of the module enhanced the indoor daylight by 7% compared to the Timing One.
- iii. Timing Three: The timing position P0.6 demonstrated a great potential in raising the daylight level in all hours especially in June (HOY: 4116) while indoor illuminance threshold reached its maximum value by almost 16.08% of the grid. This outcome enabled deeper daylight into the space in other time zones whereas there is a higher risk of receiving uncomfortable direct sunlight.

Based on the results shown in Fig. 13, timing modes proved the observation for obtaining wide range of indoor daylight with

consideration of different material specifications. Moreover, within all timing patterns of June (HOY: 4116), once the sun position represents a higher altitude, Kaleidocycle modules enhance the shading role in the summer, while the same modes provided more daylight into interior spaces in other time hours. As a general trend, it is also noticed that regardless of the sun angle, opening fraction of the modules could increase daylight penetration where selected outputs indicate a high privilege to maximize or minimize the indoor daylight based on hourly timing settings and user demand.

The second main aspect that affects the daylighting, and was fully considered in the simulation process is the use of different transparency settings via applying five sun shaded material compositions as transmittance fabrics (Table 2). Based on the selected timing positions as the most effective skin configurations in daylight harvesting simulated in Fig. 13, Fig. 14 illustrates the material selection impact on indoor illuminance in December (HOY: 8508) as a case study. Particularly, 'Season-White' could bring more daylight, while 'Palmetto-Black' provided higher shading feature in light of the least reflections compared to the other fabrics. RGB reflectance played a significant role in

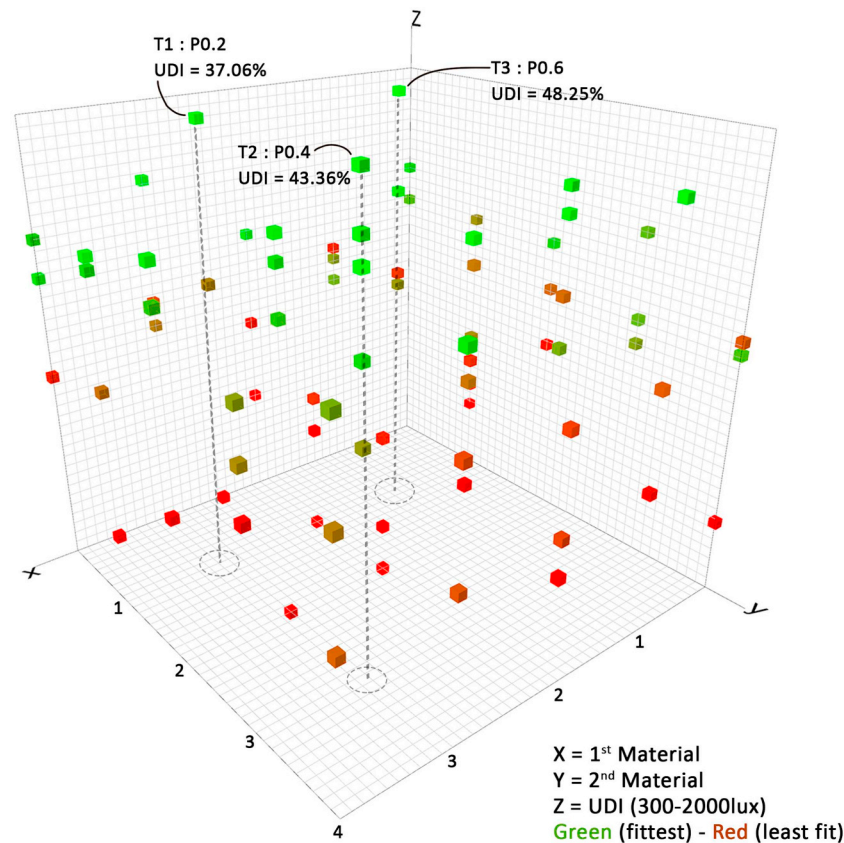


Fig. 14. Maximum UDI value based on fabric variables in P0.2, P0.4 and P0.6 of T1, T2 and T3 respectively (HOY: 8508).

redirecting light into the space when the shade is almost in the compressed position.

Subsequently, in T1:P0.2, T2:P0.4 and T3:P0.6, the acceptable incoming daylight (UDI) is respectively increased up to 7%, 7% and 5% of the grid, vs the modules' transmissivity, while $UDI_{overlit}$ remains constant. Unlikely, in the widest Kaleidocycle position (P1) and except for Timing One which is more planar compared to Timing Two and Three, the results are mostly depending on specular transmission factor of the fabric. Therefore, visual light penetration of the selected shading materials could gradually raise the indoor daylight on the task plane especially from $UDI_{underlit}$ domain to the acceptable range (300–2000 lx) if there is a logical combination between transmission and reflectance due to the shading state. Henceforth, an integration between “Season-White” and “Palmetto-Black” is recommended to cover all possible positions that are applied to evaluate discomfort glare.

4.3. Glare and view fields

DGP is considered as a generalizable glare index since it, simultaneously, takes into account the overall brightness of the view fields while DGI is a short-term index based on subjective ratings from human subjects. Therefore, DGP and DGI are evaluated in the following selected generations which are divided based on Timing patterns among three adjusted indoor view angles in an accurate rendering resolution as specified in Table 4. Module geometrical proportions and view inclination towards the screen are considered as the main influential factors that define the acceptable ratio of indoor illuminance and glare discomfort, respectively.

Fig. 15 shows an obvious improvement in terms of describing the resultant dataset over the previous responsive skin prototypes. However, it cannot be safely assumed that it can demonstrate the same effectiveness in other Timing patterns subject to slightly different setups.

This is an inevitable characteristic of comfort related regression approaches as a practical factor that can affect the results, causing a metric to over- or underperform in different attempts. Specifically, the overall performance of each timing pattern and its individual positions on the glare probability deliver a potential for users to choose the desired alternatives in order to provide proper indoor visual environment. As previously selected, T1:P0.2, T2:P0.4 and T3:P0.6 were able to bring the most sunlight into the workstation in which they could enhance glare discomfort ranges as well. In Fig. 15, DGP of all view angles are sorted based on the maximum values where the user perspective towards outdoor (DGP1 and DGI1) is evaluated for each HOY.

The leading aspect of this analysis is developed based on three suggested view fields, while the factors including ‘Monitor view’ and ‘45 Degrees towards outdoor’ did not experience DGP above 0.35. These findings are corroborated even if subject to the high quantity of indoor daylight by achieving the illuminance threshold of 300 lx within 65% of working plane area (T3:P0.6). In fact, the prototype could propose a new solution towards a challenging task to achieve glare comfort index in view field of ‘Towards outdoor’. In fact, fabrics of high openness could result in higher order magnitudes of luminance, while the user can keep his outdoor visual connection. Moreover, as an overall performance of material selections based on Fig. 14, it is proved that choosing cloth material with the least reflection property (Palmetto-Black) and allowing sunlight penetration through diffuse transmission or RGB reflection capability (Season-White) of Kaleidocycle modules are integrated solutions on controlling glare discomfort.

Table 4

Accurate rendering settings.

Ambient bounces: 6 – ambient division: 1024 – ambient resolution: 64 – ambient accuracy: 0.15 – ambient super-samples: 256



Fig. 15. Glare probability of different view fields.

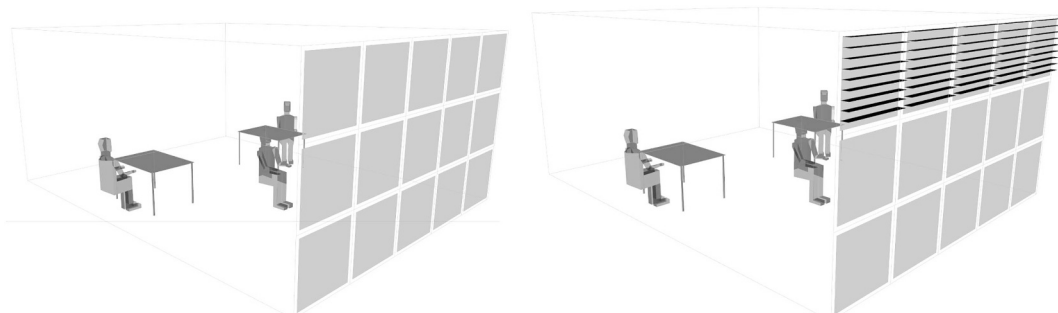


Fig. 16. Unshaded (left); Venetian blinds (right).

5. Comparison and findings

Previous research studies on conventional shading systems such as smart glazing, venetian blinds, roller shades or light shelves, that can be located internally or externally, showed that the most popular device is venetian blinds among. Hence, the proposed Kaleidocycle overall performance is compared with two shading assumptions as depicted in Fig. 16: (1) an Unshaded façade and (2) applying static external Venetian Blinds with 2 m height from the threshold going to the top with 1 mm of thickness, 10 cm length and 90% reflectivity [57,58]. In addition, the performance results are only conducted for the “Towards Outdoor” perspective in 21st of each month (Clear Sky) during working hours (7 a.m. to 16 p.m.) in a high-quality setting (Table 4).

Tables 5 and 6 examine the advantages and drawbacks of each operation criteria to achieve the optimum visual comfort at each time step in 21st of March and September which resulted in a similar performance. Based on that, DGP values; higher than 0.35 are extracted as critical hours (9 a.m. to 14 p.m.) in which the user experiences perceptible and disturbing glare with a high rate of $UDI_{overlit}$ under “Unshaded” condition. So, Kaleidocycle modules and their hourly timing patterns are selected to minimize discomfort glare and $UDI_{overlit}$ as an overall approach and accordingly, the designated modules could control unwanted indoor daylight above 2000 lx. This keeps $UDI > 55\%$ of the task area during user presence while DGP is beyond acceptable range in critical hours as opposed to the indoor illuminance performance of venetian blinds.

In the 21st of June, there are no critical elements during working hours, therefore Kaleidocycle patterns are positioned to maximize UDI while keeping DGP below perceptible range. As shown in Table 7, within studied Kaleidocycle motion patterns in this research, Timing Three has the advantage of changing indoor illuminance variation above 2000 lx to the desired range. This is again advantageous in comparison with venetian blinds especially in a range from 10 a.m. to 13 p.m. when the sun altitude is high.

As revealed in Table 8, glare discomfort reaches intolerable threshold within critical hours in 21st of December, in which almost 50% of the task area receives above 2000 lx. Using typical venetian blinds could not satisfy users in an acceptable glare probability range, however applying Kaleidocycle modules in their most shaded position provides higher useful indoor daylight in the meanwhile of keeping glare discomfort below perceptible glare.

Table 5
Performance comparison in March 21st.

Working hour	Unshaded skin		Venetian blinds		Kaleidocycle module		
	DGP1/ DGI1	UDI/ UDI(overlit)	DGP1/ DGI1	UDI/ UDI(overlit)	DGP1/ DGI1	UDI UDI(overlit)	Timing/state
7 A.M.	0.26/ 17.09	56.64/ 7.69	0.25/ 17.96	48.95/ 7.69	0.28/ 21.00	59.44/ 0	T3/P0.6
8 A.M.	0.33/ 17.14	83.19/ 16.08	0.30/ 17.63	83.21/ 10.48	0.31/ 22.40	63.63/ 0	T2/P0.6
Critical hours	9 A.M.	0.38/ 15.23	0.34/ 16.91	81.81/ 18.18	0.34/ 23.77	75.52/ 1.39	T1/P0.8
	10 A.M.	0.4/ 0	0.36/ 13.21	79.02/ 20.97	0.34/ 24.18	66.43/ 4.19	T1/P0.4
	11 A.M.	0.4/ 0	0.36/ -- 10.47	77.62/ 22.37	0.36/ 22.12	90.2/ 9.79	T1/P0.2
	12 P.M.	0.4/ 0	0.36/ -- 11.73	77.62/ 22.37	0.35/ 24.48	69.93/ 6.29	T1/P0
	13 P.M.	0.4/ 0	0.36/ 11.64	78.32/ 21.67	0.31/ 23.45	54.54/ 4.14	T3/P1
	14 P.M.	0.38/ 9.41	0.36/ 16.23	79.72/ 20.27	0.34/ 23.78	77.62/ 1.39	T1/P0.8
	15 P.M.	0.34/ 16.33	0.31/ 17.21	84.61/ 13.98	0.31/ 23.02	64.33/ 0	T2/P0.8
	16 P.M.	0.28/ 16.76	0.27/ 17.54	59.44/ 9.09	0.33/ 21.92	73.42/ 2.79	T3/P0.6

Studying the quantitative data provides more insight as well. The variation of the indoor illuminance quantities, and their impact on users' visual comfort are compared within three performance criteria based on glare indices. One of the barriers in the utilization of computer-based simulation in practice is the computation time. The point in time simulations in this paper are performed using a PC (Intel Core i7 CPU at 2.20 GHz and 8GB RAM) with Radiance (version 5.1.0). Therefore, it is neither feasible nor useful to illustrate the year-long database (8760 images) especially when the proposed prototype is able to change at each time step.

As a result, the recorded DGP values in four days during working hours ranged from 0.25 to 1.0 and DGI values ranged from −16.97 to 37.92 (surprisingly, DGI values are technically possible) within critical hours. Since, DGP is strongly weighted on vertical illuminance, it always reported disturbing glare in a brightly lit workspace when the façade is unshaded. Conversely, the DGI is reported in a comfortable range even when it directly faces the outdoor. This is due to the average luminance term in Eq. (3), in which the background luminance term causes DGI to drop as the background luminance increases. The results show no correlation between DGI and subjective glare assessment which is fully conformed with literature [32]. Thus, there is less confidence in DGI as a metric for assessing the glare in contrast to DGP which denotes stronger correlation with users' response regarding glare perception in its dataset.

6. Conclusion

Drawn by the gap in the body of knowledge to achieve flexible shading systems via smart ASFs, an origami-based hexagonal adaptive solar skin was developed using a single office workstation located in Tehran, as the testbed of this study. Progressively, a parametric approach was introduced and employed where three Timing curves were designed as research developing methods to analyse point-in-time illuminance and glare probability. Geometrical properties of all timings were extracted from the field measurements as well as their material settings and were applied in simulations. Around 1800 design models were conducted during the simulation by an environmental plug-in Honeybee to improve the indoor daylight performance regarding correlations between geometrical attributes and orientations of screen positions with comfort glare adjustment.

In terms of the optimization dataset, two resolution settings as

Table 6
Performance comparison in September 21st.

Working hour		Unshaded skin		Venetian blinds		Kaleidocycle module		
		DGP1/ DGI1	UDI/ UDI(overlit)	DGP1/ DGI1	UDI/ UDI(overlit)	DGP1/ DGI1	UDI/ UDI(overlit)	Timing/state
7 A.M.		0.28/ 17.15	63.63/ 8.39	0.26/ 17.73	56.64/ 6.29	0.31/ 21.57	68.53/ 0	T3/P0.6
8 A.M.		0.34/ 16.88	81.81/ 18.18	0.31/ 17.43	85.31/ 13.28	0.32/ 22.66	72.72/ 0	T3/P0.2
Critical hours	9 A.M.	0.38/ 9.57	74.12/ 25.87	0.34/ 16.51	81.81/ 18.18	0.35/ 23.08	85.31/ 10.48	T2/P0.6
		0.4/ 0	70.62/ 29.37	0.36/ 11.64	78.32/ 21.67	0.33/ 23.89	67.83/ 3.49	T1/P0.6
	11 A.M.	0.4/ 0	69.93/ 30.06	0.36/ −13.87	77.62/ 22.37	0.34/ 23.37	67.13/ 6.99	T1/P0.6
		0.4/ 0	69.93/ 30.06	0.36/ −16.97	77.62/ 22.37	0.34/ 23.63	70.62/ 6.99	T1/P0.4
	13 P.M.	0.39/ 0	71.32/ 28.67	0.36/ 12.76	78.32/ 21.67	0.33/ 24.19	66.43/ 0	T1/P0.4
		0.37/ 14.57	74.12/ 25.87	0.34/ 16.43	81.11/ 18.88	0.33/ 22.94	79.02/ 0	T1/P0.2
	15 P.M.	0.32/ 16.55	82.51/ 17.48	0.30/ 17.31	83.21/ 13.28	0.35/ 23.08	89.51/ 7.69	T3/P0.4
		0.27/ 16.75	69.23/ 8.39	0.26/ 17.64	55.94/ 5.59	0.33/ 22.16	59.44/ 0	T3/P0.4

‘medium’ and ‘accurate’ were implemented based on Tables 3 and 4 respectively. With respect to ‘medium’ resolution employed for Timing 2, the correlations between UDI domains and Glare indices (DGP and DGI) were indicated within three view fields depending on the several variable expressions. Except for June that tested configurations played a significant role in shading interior, there are few optimum solutions that could address the main visual comfort requirements. It is constrained to the minimum of 50% of the task where position 0.2 and 0.4 of Timing Two can be selected as the most favourable configurations, however it depends on the user preference during working hours.

Applying parametric analysis contributed to generating design models for the internal daylighting conditions, and adjusting the hexagonal ASF for the visual comfort of occupants. Furthermore, the hUDI was achieved within the defined standard range of > 300 lx in percentage. It was also deduced that regardless of the sun angle, opening fraction of the modules could increase daylight penetration where

selected outputs indicate a high privilege to maximize or minimize the indoor daylight based on hourly timing settings and user demand. Regarding the transparency settings, an integration between “Season-White” and “Palmetto-Black” was derived to cover all possible positions that are applied to evaluate discomfort glare.

Thanks to the Kaleidocycle module positions, results reveal that using the positions with high openness has a positive effect on illuminance, but also a negative impact on the glare only in selected indoor view fields. Significantly, it can be adjusted by choosing a proper timing-based skin configuration for a glare-free daylight. The findings also confirmed that applying the proposed Timing patterns over a responsive skin could deliver incoming daylight enhancement and shading possibility along with controlling DGP and DGI indices of glare based on the user preference and productivity at any hour of the day.

The comparison of the prototype with two different scenarios of unshaded façade and external Venetian Blinds further distinguished the

Table 7
Performance comparison in June 21st.

Working hour	Unshaded skin		Venetian blinds		Kaleidocycle system		
	DGP1/ DGI1	UDI/ UDI(overlit)	DGP1/ DGI1	UDI/ UDI(overlit)	DGP1/ DGI1	UDI/ UDI(overlit)	Timing/state
7 A.M.	0.27/ 18.64	65.73/ 0	0.27/ 19.21	63.63/ 0	0.25/ 18.94	47.55/ 0	T3/P0.6
8 A.M.	0.28/ 16.25	89.51/ 0	0.28/ 17.49	82.51/ 0	0.26/ 18.83	58.74/ 0	T3/P0.6
9 A.M.	0.29/ 13.03	93.00/ 5.59	0.29/ 15.05	97.90/ 0	0.30/ 19.90	80.41/ 0	T3/P0.6
10 A.M.	0.30/ 6.72	86.71/ 13.28	0.30/ 12.57	90.90/ 9.09	0.32/ 19.68	88.81/ 9.79	T3/P0.6
11 A.M.	0.32/ 0	81.81/ 18.18	0.31/ 11.98	85.31/ 14.68	0.34/ 20.93	100/ 0	T3/P0.4
12 P.M.	0.32/ 0	79.72/ 20.27	0.32/ 13.00	85.31/ 14.68	0.35/ 20.81	99.30/ 0	T3/P0.4
13 P.M.	0.30/ 5.04	86.01/ 13.98	0.30/ 12.48	88.81/ 11.18	0.33/ 20.88	95.80/ 0	T3/P0.4
14 P.M.	0.29/ 12.76	89.51/ 9.79	0.29/ 14.78	95.80/ 2.79	0.30/ 20.64	74.82/ 0	T3/P0.4
15 P.M.	0.28/ 16.17	93.00/ 0	0.28/ 17.26	90.20/ 0	0.27/ 19.08	62.93/ 0	T3/P0.6
16 P.M.	0.27/ 18.52	69.23/ 0	0.27/ 19.00	65.73/ 0	0.25/ 18.85	51.04/ 0	T3/P0.6

Table 8
Performance comparison in December 21st.

Working hour		Unshaded skin		Venetian blinds		Kaleidocycle module		Timing/state
		DGP1/ DGI1	UDI/ UDI(overlit)	DGP1/ DGI1	UDI/ UDI(overlit)	DGP1/ DGI1	UDI/ UDI(overlit)	
7 A.M.		0.25/ 13.72	67.8 /10.48	0.25/ 14.35	65.03/ 9.09	0.27/ 20.10	60.13/ 0	T3/P0.6
8 A.M.		0.34/ 16.99	66.43/ 33.56	0.33/ 16.82	67.83/ 32.16	0.33/ 22.99	74.12/ 5.59	T3/P0.8
Critical hours	9 A.M.	1/ 37.11	57.34/ 42.65	1/ 37.12	63.63/ 36.36	0.38/ 25.94	79.02/ 2.79	T1/P0
	10 A.M.	1/ 37.92	53.14/ 46.85	1/ 36.54	65.73/ 34.26	0.42/ 25.13	81.11/ 18.88	T1/P0
	11 A.M.	1/ 37.60	48.95/ 51.04	1/ 35.81	65.03/ 34.94	0.35/ 24.22	72.72/ 15.38	T1/P0
	12 P.M.	0.46/ 18.18	48.95/ 51.04	0.43/ 18.95	67.83/ 32.16	0.35/ 23.29	79.72/ 14.68	T1/P0.4
	13 P.M.	1/ 37.86	53.14/ 46.85	0.43/ 18.53	66.43/ 33.56	0.38/ 24.29	79.72/ 18.88	T1/P0
	14 P.M.	1/ 37.34	55.24/ 44.75	1/ 36.41	62.93/ 37.06	0.38/ 25.78	81.81/ 2.79	T1/P0
	15 P.M.	0.34/ 16.16	65.03/ 34.96	0.32/ 17.06	65.73/ 34.26	0.35/ 24.28	77.62/ 0.69	T3/P0.2
	16 P.M.	0.25/ 14.44	66.93/ 13.28	0.25/ 15.12	62.93/ 12.58	0.27/ 19.70	60.83/ 0.69	T3/P0.6

positive performance in 'accurate' simulation resolution in daylighting and minimizing glares. Interestingly, it was also found out that there is less confidence in DGI mostly in highly-illuminated cases as a metric for assessing the glare as opposed to DGP which indicates stronger correlation with users' response regarding glare perception in its dataset. Notwithstanding the contributions made, there are some limitations to be acknowledged. First, the optimization solutions were run as the extreme indications of four-time steps during a year as indicators that are covering the whole possible different circumstances during a year. This approach could present the sense of prototype flexibility for the other time intervals. However, the authors acknowledge that this is an unavoidable limitation of the study. Second, the findings should be treated with caution in direct application to real-life buildings, given that the data were collected through generating a fictitious office space. Third, the performance of the developed algorithm is open to enhancement to reach the minimum discomfort in the interim of maximizing the visual comfort. This particular approach is of potential to be investigated in many possible diverse Timing trends or time hours corresponding with lower sun angles to meet the visual performance requirements. Therefore, more accurate results require more cases to be considered in the evaluation that can be conducted as future works. The design recommendation in this study can be employed in different climates with conducting the same procedure for further assessments.

References

- [1] M. Arif, M. Katafygiotou, A. Mazroei, A. Kaushik, E. Elsarrag, Impact of indoor environmental quality on occupant well-being and comfort: a review of the literature, *International Journal of Sustainable Built Environment* 5 (1) (2016) 1–11 <https://doi.org/10.1016/j.ijsbe.2016.03.006>.
- [2] S. Attia, S. Bilir, T. Safy, C. Struck, R.C.G.M. Loonen, F. Goia, Current trends and future challenges in the performance assessment of adaptive façade systems, *Energy and Buildings* 179 (2018) 165–182 <https://doi.org/10.1016/j.enbuild.2018.09.017>.
- [3] S. Attia, F. Favoino, R. Loonen, A. Petrovski, A. Monge-Barrio, Adaptive façades system assessment: an initial review, 10th Conference on Advanced Building Skins, Bern, Switzerland, 2015, pp. 1265–1273 (3981205383), <http://hdl.handle.net/2268/187576>.
- [4] S. Banihashemi, G. Ding, J. Wang, Developing a hybrid model of prediction and classification algorithms for building energy consumption, *Energy Procedia* 110 (2017) 371–376, <https://doi.org/10.1016/j.egypro.2017.03.155>.
- [5] S. Banihashemi, H. Golizadeh, M.R. Hosseini, M. Shakouri, Climatic, parametric and non-parametric analysis of energy performance of double-glazed windows in different climates, *International Journal of Sustainable Built Environment* 4 (2) (2015) 307–322 <https://doi.org/10.1016/j.ijsbe.2015.09.002>.
- [6] S. Banihashemi, M.S. Hassanabadi, A.N. Sadeghifam, Analysis of behavior of windows in terms of saving energy in extreme cold weather climates of Iran, *International Journal of Engineering and Technology* 4 (6) (2012) 460. 1793–8236, <https://doi.org/10.7763/IJET.2012.V4.460>.
- [7] S. Banihashemi, A. Tabadkani, M.R. Hosseini, Integration of parametric design into modular coordination: a construction waste reduction workflow, *Autom. Constr.* 88 (2018) 1–12 <https://doi.org/10.1016/j.autcon.2017.12.026>.
- [8] S. Banihashemi, A. Tabadkani, M.R. Hosseini, Modular coordination-based generative algorithm to optimize construction waste, *Procedia Engineering* 180 (2017) 1877–1885, <https://doi.org/10.1016/j.proeng.2017.04.222>.
- [9] M. Barozzi, J. Lienhard, A. Zanelli, C. Monticelli, The sustainability of adaptive envelopes: developments of kinetic architecture, *Procedia Engineering* 155 (2016) 1877–1885, <https://doi.org/10.1016/j.proeng.2016.08.029>.
- [10] L. Bellia, A. Cesarano, G.F. Iuliano, G. Spada, Daylight glare: a review of discomfort indexes, *Visual Quality and Energy Efficiency in Indoor Lighting: Today for Tomorrow*, Roma, Italia, 2008 <http://www.fedoa.unina.it/1312/>.
- [11] Y. Bian, T. Leng, Y. Ma, A proposed discomfort glare evaluation method based on the concept of 'adaptive zone', *Build. Environ.* 3601323 (143) (2018) 306–317, <https://doi.org/10.1016/j.buildenv.2018.07.025>.
- [12] B. Bueno, J.M. Cejudo-López, A. Katsifarakis, H.R. Wilson, A systematic workflow for retrofitting office façades with large window-to-wall ratios based on automatic control and building simulations, *Build. Environ.* 132 (104–113) (2018) 3601323, <https://doi.org/10.1016/j.buildenv.2018.01.031>.
- [13] S. Carlucci, F. Causone, F. De Rosa, L. Pagliano, A review of indices for assessing visual comfort with a view to their use in optimization processes to support building integrated design, *Renew. Sust. Energ. Rev.* 47 (2015) 1016–1033 <https://doi.org/10.1016/j.rser.2015.03.062>.
- [14] CEN, EN 12464-1: light and lighting-lighting of work places, part 1: indoor work places, 5/03/2018, 2002. <https://standards.globalspec.com/std/1380223/en-12464-1>.
- [15] P. Chauvel, J. Collins, R. Dogniaux, J. Longmore, Glare from windows: current views of the problem, *Lighting Research & Technology* 14 (1) (1982) 31–46 <https://doi.org/10.1177/0013790218201400103>.
- [16] K. Cilento, Al Bahar Towers Responsive Facade/aedas, 5 ArchDaily, 2012, pp. 0719–8884 <https://www.archdaily.com/270592/al-bahar-towers-responsive-facade-aedas/>.
- [17] Y. Elghazi, A. Mahmoud, Origami explorations a generative parametric technique for kinetic cellular façade to optimize daylight performance, 34th Computer Aided Architectural Design Conference, vol. 2, University of Oulu, 2016, pp. 399–408 http://papers.cumincad.org/data/works/att/ecaade2016_007.pdf.
- [18] A. Eltaweel, Y. Su, Controlling venetian blinds based on parametric design: via implementing Grasshopper's plugins: a case study of an office building in Cairo, *Energy and Buildings* 139 (2017) 31–43 <https://doi.org/10.1016/j.enbuild.2016.12.075>.
- [19] A. Eltaweel, S. Yuehong, Parametric design and daylighting: a literature review, *Renew. Sust. Energ. Rev.* 73 (2017) 1086–1103 <https://doi.org/10.1016/j.rser.2017.02.011>.
- [20] A. Eltaweel, S. Yuehong, Using integrated parametric control to achieve better daylighting uniformity in an office room: a multi-step comparison study, *Energy and Buildings* 152 (2017) 137–148 <https://doi.org/10.1016/j.enbuild.2017.07.033>.
- [21] A. Galatioto, M. Beccali, Aspects and issues of daylighting assessment: a review

- study, *Renew. Sust. Energ. Rev.* 66 (2016) 852–860 1364-0321 <https://doi.org/10.1016/j.rser.2016.08.018>.
- [22] J.Y. Garretón, R.G. Rodríguez, A. Ruiz, A.E. Pattini, Degree of eye opening: a new discomfort glare indicator, *Build. Environ.* 88 (2015) 142–150 0360-1323 <https://doi.org/10.1016/j.buildenv.2014.11.010>.
- [23] D. Hafiz, Daylighting, space, and architecture: a literature review, *Enquiry: A Journal for Architectural Research* 12 (1) (2015) 2329–9339, <https://doi.org/10.17831/enq:arcc.v12i1.391>.
- [24] M.S. Hassanabadi, S. Banihashemi, A.R. Javaheri, Analysis and comparison of impacts of design optimization approaches with occupant behavior on energy consumption reduction in residential buildings, *International Journal of Engineering and Technology* 4 (6) (2012) 680 1793-8236 <https://doi.org/10.7763/IJET.2012.V4.461>.
- [25] B. Hasselaar, Climate adaptive skins: towards the new energy-efficient façade, *WIT Trans. Ecol. Environ.* 99 (2006) 351–360, <https://doi.org/10.2495/RAV060351>.
- [26] R.G. Hopkinson, Glare from daylighting in buildings, *Appl. Ergon.* 3 (4) (1972) 206–215 0003-6870 [https://doi.org/10.1016/0003-6870\(72\)90102-0](https://doi.org/10.1016/0003-6870(72)90102-0).
- [27] Insolroll, Window shading systems manufacturer, <https://insolroll.com/>, (2018).
- [28] A. Kirimtat, B.K. Koyunbaba, I. Chatzikonstantinou, S. Sariyildiz, Review of simulation modeling for shading devices in buildings, *Renew. Sust. Energ. Rev.* 53 (2016) 23–49 1364-0321 <https://doi.org/10.1016/j.rser.2015.08.020>.
- [29] K. Kurnia, D. Azizah, R. Mangkuto, R. Atmodipoeoro, Visual comfort assessment using high dynamic range images under daylight condition in the main library building of Institut Teknologi Bandung, *Procedia engineering* 234-239 (170) (2017) 1877–7058, <https://doi.org/10.1016/j.proeng.2017.03.056>.
- [30] R.C.G.M. Loonen, M. Trčka, D. Cóstola, J.L.M. Hensen, Climate adaptive building shells: state-of-the-art and future challenges, *Renew. Sust. Energ. Rev.* 25 (2013) 483–493 1364-0321 <https://doi.org/10.1016/j.rser.2013.04.016>.
- [31] J. Mardaljevic, M. Andersen, N. Roy, J. Christoffersen, Daylighting metrics: is there a relation between useful daylight illuminance and daylight glare probability, *Proceedings of the Building Simulation and Optimization Conference (BSO12)*, Loughborough, UK, 1011 2012, pp. 2522–2708 <http://www.ibpsa.org/proceedings/BSO2012/3B1.pdf>.
- [32] A. McNeil, G. Burrell, Applicability of DGP and DGI for evaluating glare in a brightly daylight space, *Proceedings of Simulation Building*, 6 International Building Performance Simulation Association, Salt Lake City, USA, 2016, pp. 2522–2708 <http://ibpsa.usa.org/index.php/ibpsa/article/view/339/328>.
- [33] A. Michelle, S. Daniel, *Smart Materials and New Technologies for the Architecture and Design Professions*, Elsevier, Architectural Press, Oxford, 2005 (0750662255).
- [34] J. Moloney, *Designing Kinetics for Architectural Facades: State Change*, Routledge, 2011 (1136709045).
- [35] Z. Nagy, B. Svetozarevic, P. Jayathissa, M. Begle, J. Hofer, G. Lydon, A. Willmann, A. Schlueter, The adaptive solar facade: from concept to prototypes, *Frontiers of Architectural Research* 5 (2) (2016) 143–156 2095-2635 <https://doi.org/10.1016/j.foar.2016.03.002>.
- [36] K. Panopoulos, A. Papadopoulos, Smart facades for non-residential buildings: an assessment, *Advances in Building Energy Research* 11 (1) (2017) 26–36 1751-2549 <https://doi.org/10.1080/17512549.2015.1119058>.
- [37] C.-S. Park, Occupant Responsive Optimal Control of Smart Façade Systems, Georgia Institute of Technology, 2003 10/03/2018 https://smartechn.gatech.edu/bitstream/handle/1853/9450/Park_Cheolsoo_200308_phd.pdf.
- [38] C.-S. Park, G. Augenbroe, T. Messadi, Daylighting optimization in smart facade systems, *Proceedings of the Eighth International IBPSA Conference*, 2003, pp. 2522–2708 (doi:10.1.1.472.7157).
- [39] E.A. Peraza-Hernandez, D.J. Hartl, R.J. Malak Jr., D.C. Lagoudas, Origami-inspired active structures: a synthesis and review, *Smart Mater. Struct.* 23 (9) (2014) 0964–1726, <https://doi.org/10.1088/0964-1726/23/9/094001> 094001.
- [40] M. Pesenti, G. Masera, F. Fiorito, M. Sauchelli, Kinetic solar skin: a responsive folding technique, *Energy Procedia* 70 661-672 (2015) 1876–6102, <https://doi.org/10.1016/j.egypro.2015.02.174>.
- [41] Radiance 2.4, Setting rendering options, https://floyd.lbl.gov/radiance/refer/Notes/rpict_options.html.
- [42] R.G. Rodríguez, J.A.Y. Garretón, A.E. Pattini, An epidemiological approach to daylight discomfort glare, *Build. Environ.* 113 (2017) 39–48 0360-1323 <https://doi.org/10.1016/j.buildenv.2016.09.028>.
- [43] R.G. Rodríguez, J.A. Yamín Garretón, A.E. Pattini, An epidemiological approach to daylight discomfort glare, *Build. Environ.* 113 (39–48) (2017) 3601323, <https://doi.org/10.1016/j.buildenv.2016.09.028>.
- [44] M.S. Roudsari, M. Pak, A. Smith, Ladybug: a parametric environmental plugin for grasshopper to help designers create an environmentally-conscious design, *Proceedings of the 13th International Building Performance Simulation Association Lyon, France, 2013*, pp. 2522–2708 http://www.ibpsa.org/?page_id=349.
- [45] N. Ruck, S. Selkowitz, Q. Aschehoug, J. Christoffersen, R. Jakobiak, K. Johnsen, E. Lee, *Daylight in buildings: a source book on daylighting systems and components*, Lawrence Berkeley National Laboratory (2000) 9910-47493.
- [46] D. Rutten, Evolutionary principles applied to problem solving using Galapagos, *Advances in Architectural Geometry*, 2010 Vienna. 978-3-902233-03-5 <http://www.architecturalgeometry.org/aag10/index.php>.
- [47] D. Rutten, Galapagos: on the logic and limitations of generic solvers, *Archit. Des.* 83 (2) (2013) 132–135 0003-8504 <https://doi.org/10.1002/ad.1568>.
- [48] A.H. Sadek, R. Mahrous, Adaptive glazing technologies: balancing the benefits of outdoor views in healthcare environments, *Sol. Energy* 174 (2018) 719–727 0038-092X <https://doi.org/10.1016/j.solener.2018.09.032>.
- [49] C. Sapia, Daylighting in buildings: developments of sunlight addressing by optical fiber, *Sol. Energy* 89 (2013) 113–121 0038-092X <https://doi.org/10.1016/j.solener.2012.12.003>.
- [50] M. Shakouri Hassanabadi, S. Banihashemi, Developing an empirical predictive energy-rating model for windows by using Artificial Neural Network, *International Journal of Green Energy* (2012) 1543–5075, <https://doi.org/10.1080/15435075.2012.738451>.
- [51] F. Soflaei, M. Shokouhian, H. Abraveshdar, A. Alipour, The impact of courtyard design variants on shading performance in hot-arid climates of Iran, *Energy and buildings* 143 (2017) 71–83 0378-7788 <https://doi.org/10.1016/j.enbuild.2017.03.027>.
- [52] C. Struck, M.G. Almeida, S.M. Silva, R. Mateus, P. Lemarchand, A. Petrovski, R. Rabenseifer, R. Wandsronk, F. Wellershoff, J. De Wit, Adaptive facade systems – review of performance requirements, design approaches, use cases and market needs, *10th Energy Forum on Advanced Building Skins*, 1 2015, <https://doi.org/10.13140/RG.2.1.2023.8165> Bern.
- [53] J.Y. Suk, M. Schiler, K. Kensek, Absolute glare factor and relative glare factor based metric: predicting and quantifying levels of daylight glare in office space, *Energy and buildings* 130 (2016) 8–19 0378-7788 <https://doi.org/10.1016/j.enbuild.2016.08.021>.
- [54] J.Y. Suk, M. Schiler, K. Kensek, Investigation of existing discomfort glare indices using human subject study data, *Build. Environ.* 113 (2017) 121–130 0360-1323 <https://doi.org/10.1016/j.buildenv.2016.09.018>.
- [55] R. Suralkar, Solar Responsive Kinetic Facade Shading Systems Inspired by Plant Movements in Nature, 1st Conference of People and Buildings, Network for Comfort and Energy Use in Buildings, London, UK, 2011 <http://nceub.commoncense.info/index.php?n=Network.MC2011ConferencePapers>.
- [56] A. Tabadkani, S. Banihashemi, M.R. Hosseini, Daylighting and visual comfort of oriental sun responsive skins: a parametric analysis, *Build. Simul.* 11 (4) (2018) 663–676 1996-3599 <https://doi.org/10.1007/s12273-018-0433-0>.
- [57] A. Tabadkani, M. Valinejadshoubi, Smart Transformable Shading System With Adaptability to Climate Change, *United States Patent and Trademark Office (USPTO)* (Ed.), United States, 2018 <https://patents.google.com/patent/US20180216399A1/en?inventor=Seyed+Amir+Tabadkani>.
- [58] M.M. Tahmasebi, S. Banihashemi, M.S. Hassanabadi, Assessment of the variation impacts of window on energy consumption and carbon footprint, *Procedia engineering* 21 (2011) 820–828 1877-7058 <https://doi.org/10.1016/j.proeng.2011.11.2083>.
- [59] T. Tomasetti, Design explorer, <http://tt-acm.github.io/DesignExplorer>, (2017).
- [60] J. Wienold, J. Christoffersen, Evaluation methods and development of a new glare prediction model for daylight environments with the use of CCD cameras, *Energy and buildings* 38 (7) (2006) 743–757 0378-7788 <https://doi.org/10.1016/j.enbuild.2006.03.017>.